TAMPEREEN TEKNILLINEN YLIOPISTO
TAMPERE UNIVERSITY OF TECHNOLOGY

VIDISHA NAIK

Selecting an Appropriate Curvature Sensor for Fluidic Soft Robot and Modeling Sensor Reading vs Pressure vs Position

Master of Science Thesis

Examiner: Prof. Reza Ghabcheloo
Examiner and topic approved by the Faculty Council of the Faculty of Engineering Sciences on 9th August 2017

ABSTRACT

VIDISHA NAIK: Selecting an Appropriate Curvature Sensor for Fluidic Soft Robot and Modeling Sensor Reading vs Pressure vs Position
Tampere University of technology
Master of Science Thesis, 54 pages
October 2017
Master's Degree Programme in Automation Engineering
Major: Factory Automation and Industrial Informatics
Examiner: Professor Reza Ghabcheloo

Keywords: curvature sensor, soft robotics

This research focuses on the study of a curvature sensor for a fluidic soft robot. Soft robot is a complete new dimension to traditional rigid robot. A soft robot is made up of materials like Silicon, PDMS and elastomeric polymers. The actuation method can be hydraulic, pneumatic or electric. Depending on its construction, it undergoes elongation, bending, twisting, or all of the three on actuation. It brings with it some important features like compliance with the object of interaction and robustness, which is an inspiration acquired from animals and plants. This results into useful applications in fields of rehabilitation, gripping delicate objects in food industries and allowing safe interaction for humans.

The soft robot has large DOF, which allows it to maneuver in a way, which is difficult for the traditional robot. However, this large DOF makes the modeling of the soft robot for determining the robot state difficult and challenging. Another approach towards determining the robot state is using sensors. In this thesis, a thorough study is done to find out an appropriate curvature sensor to be embedded into the soft robot. The data from curvature sensor, pressure sensor and the vision system are collected in experiments undertaken with obstacles in the soft robot path. The collected data is used via machine learning technique to obtain trained model that determines the robot state and obstacle location.

PREFACE

I would like to give my sincere thanks to the Lab of Automation and Hydraulics Engineering for giving me the opportunity to conduct this research. My sincere gratitude to my thesis supervisor Prof. Reza Ghabcheloo for believing in me and providing the constant guidance and motivation, which helped me to make this Thesis. Further my thanks to doctoral student Mahdi Momeni for help in vision system calibration and Post-Doctoral student Mikko Heikkilä for constant guidance throughout thesis.

My heartfelt Thanks to my friends Salman, Aditya, Jayesh for their immense motivation. Special thanks to Ramya. Last but not the least my Mom being my emotional and motivational pillar of support.

Tampere, 25.8.2017

Vidisha Naik

Contents

1 INTRODUCTION 2
1.1 Need of Sensor & Challenges in Sensing 4
1.2 Research Objective 7
1.3 Methodology 7
2 THEORETICAL BACKGROUND 8
3 CURVATURE SENSOR ANALYSIS 13
3.1 Experimental Setup 13
3.2 Testing Flexpoint and Silver Ink curvature sensors 15
3.3 Construction and working of flex curvature sensor 17
3.4 Independent sensor calibration with 3D setup 18
3.5 Attaching sensor to soft robot 19
4 EXPERIMENTING EFFECT OF OBSTACLE ON PRESSURE vs CURVATURE SENSOR READING 23
4.1 Experimental setup 23
4.2 Preliminary tests 24
4.3 Sensor Mappings for Obstacle free case 25
4.4 Sensor Mappings in presence of Obstacles 27
5 MAPPING AND CLASSIFYING SENSOR DATA BASED ON OBSTACLES WITH MACHINE LEARNING 33
5.1 Mapping curvature and pressure sensor to robot tip y 33
5.2 Finding Instance of Obstacle Touch 36
5.2.1 Training the sensor data 36
5.2.2 Testing data on trained model 42
6 CONCLUSION 49

LIST OF FIGURES

Figure 1: Traditional robot Vs. Soft robot [4][5] 2
Figure 2: Fluidic soft robot used in the research 4
Figure 3: Kinematics in a constant curvature robot[20] 5
Figure 4: Finding tip position from arc parameters with PCC 5
Figure 5: Summary of the soft robotics in general[21] 6
Figure 6: ControlDesk interface for controller 14
Figure 7: Calibration using the GoPro camera 15
Figure 8:Flexpoint bend sensor attached to soft robot 16
Figure 9:Silver ink stretchable sensor 17
Figure 10: 3D printed setup for calibration 18
Figure 11: Bending angle Vs Sensor voltage map 19
Figure 12: Describing the low bending due to embedding sensor completely inside the robot and coating it with rubber 19
Figure 13: Failed method to attach sensor as wounding the tape caused difficulty in appropriate sensor bending 20
Figure 14: Correct attachment method for sensor 20
Figure 15: Map of Bending angle from vision (deg) vs curvature sensor reading (V) 21
Figure 16: Map of soft robot tip position y(mm) vs curvature sensor reading (V) 22
Figure 17: Soft robot with the obstacle locations 24
Figure 18: Pressure(kPa) vs Curvature sensor reading(V) 25
Figure 19: Curvature sensor reading vs time in free case 26
Figure 20: Pressure vs time 26
Figure 21: Soft robot in presence of base obstacle 27
Figure 22: Soft robot in presence of mid obstacle 28
Figure 23: Soft robot in the presence of tip obstacle 29
Figure 24: Pressure (kPa) inside soft robot vs Curvature sensor reading (V) 30
Figure 25: Deviation of base obstacle sensor values w.r.t free case 30
Figure 26:Deviation of mid obstacle sensor values w.r.t free case 31
Figure 27:Deviation of tip obstacle sensor values w.r.t free case 31
Figure 28: Description of data given to neural network 34
Figure 29: View of the created network model 34
Figure 30: Target data for base obstacle vs Predicted data obtained 35
Figure 31: Target data for mid obstacle vs Predicted data obtained 35
Figure 32: Target data for tip obstacle vs Predicted data obtained 35
Figure 33: Target data for free case vs Predicted data obtained 36
Figure 34: Selection of predictor and response 38
Figure 35: Scatter plot for pressure vs curvature sensor voltage 38
Figure 36: Selected classifier model 39

Figure 37: Confusion Matrix....39
Figure 38: ROC for free obstacle....40
Figure 39: ROC for base obstacle....40
Figure 40: ROC for mid obstacle....41
Figure 41: ROC for tip case....41
Figure 42: Target data vs predicted data for base obstacle location y (-75 mm)....43
Figure 43: Reference to identify the overlap areas....43
Figure 44: Target data vs predicted data for mid obstacle location y (-88 mm)....45
Figure 45: Reference to identify the overlap areas....45
Figure 46: Target data vs Predicted data for tip obstacle y (-110mm)....47
Figure 47: References to identify overlap areas....47

LIST OF TABLES

Table 1: Comparison based on important sensor characteristics....10
Table 2: Glove projects with flex sensor....11
Table 3: Summary of sensor and measured parameters....21
Table 4: Obstacle location y coordinate....24
Table 5: Preliminary test for voltage and pressure in free and obstacle case....25
Table 6: Summary of experiment....27
Table 7: Important observations from experiments....32
Table 8: Neural network properties selected....34
Table 9: Data given to Classifier model for learning....37
Table 10: Division of the dataset given to the Classifier model....37
Table 11: Analysis for predicted base obstacle data....44
Table 12: Analysis for predicted mid obstacle data....46
Table 13: Analysis for predicted tip obstacle data....48
Table 14: Probability of getting reliable data for each obstacle case....48

LIST OF SYMBOLS AND ABBREVIATIONS

DOF	Degree of Freedom
EGaIn	Euclectic Indium Gallium alloy
PCC	Piecewise Constant Curvature
S.P.	Set Point

1 INTRODUCTION

One of the key ingredients of any automation process is the sensing element. The more information provided by the sensors regarding the process variables, the easier it becomes to take into account parameters like disturbances, environmental interactions, which otherwise tend to make the control of a system difficult. Another benefit by sensors is safety. Sensors are deployed in almost every field like medical, industrial, space, agriculture, IOT, robotics, smart transportation etc. This research aims the study of sensor in the field of ***soft robotics***.

Soft robotics brings a shift to our imagination of robots being just the rigid body links. Soft robotics is a field of study of using soft materials, soft sensors to build up flexible manipulators[1]. The principle is inspired from the animals, plants and humans in terms of their compliance and ease of interaction with the environment[2]. "It provides a means of safer interaction with humans and unstructured environments"[3] The below Figure shows the visible difference between rigid robot and soft robot.

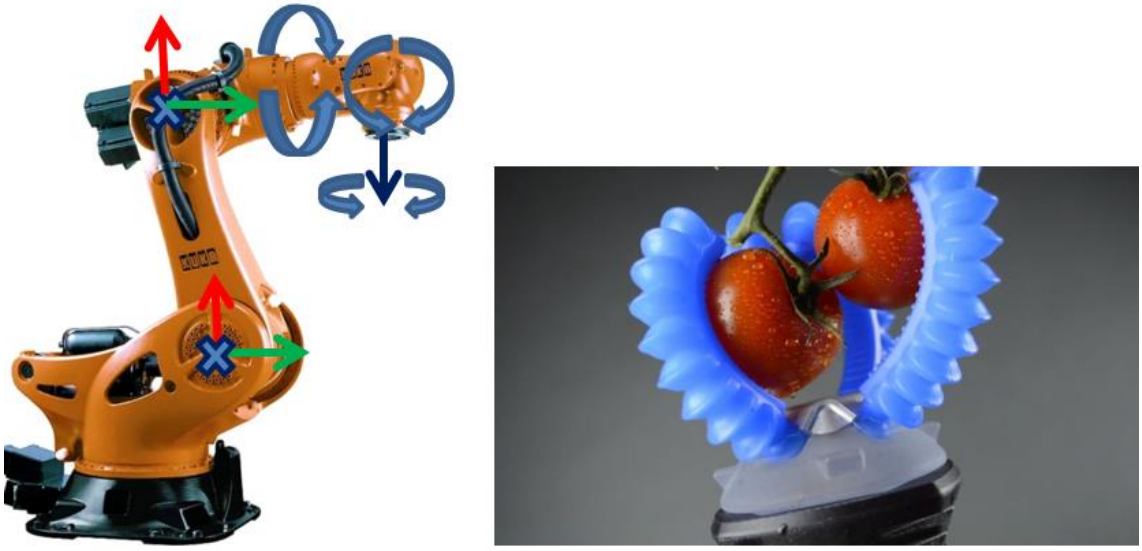

Figure 1: Traditional robot Vs. Soft robot [4][5]

The selection of materials for soft robot is such that it does not harm or impair the objects it handles. This makes rubber, silicone and polymeric materials as valid choices [6]. The materials have the ability to resemble features of biological organisms having Young's moduli as **10^4-10^9 Pa**[8]**.**This gives the advantage over traditional robot, of being able to deform and adapt easily to the object with which it interacts. Raphael et al. describes the benefit of grasping wide variety of objects due to the compliance property that is inherent in the material [9]**.**

The soft robots tend to bend, elongate, contract, stretch based on its physical structure. There are different types of actuators to enable the above states like *PneuNets* actuator comprising of elastomer with various lengths chambers [10], *Fiber-reinforced* actuator having inextensible winding of fiber around it [11], *McKibben muscles* made up of tube with braids around it [12], *Dielectric Elastomers* actuate as a response to the electric field [13].

The wide scope of soft robotic applications include developing octopus shaped robot [14], soft hands for hand rehabilitation [15], artificial eyelid closing using soft exopatch [16] . An interesting example for hand rehab using VR is presented by youGrabber[17]. A similar kind of approach is been used in soft robot hand rehab applications. The soft robot provides more advantageous in a case where a pressure can be applied on the patients hand using soft robot, which is not possible with the youGrabber. One of the most recent ongoing studies by Harvard is the pumping of heart for heart failure patients using the soft robot sleeve around heart [18].

There is also commercial manufacturing company for soft robots named Soft robotics Inc. introducing soft robotic grippers for applications in the food and beverage industries in order to handle delicate food items [19] .

The soft robot studied in this research is a fluidic soft robot as shown below in **Figure 2**. The soft robot is wound with fibers around it and thus its type is fiber reinforced soft robot. The material of the robot is PDMS which was selected out of many other materials as it provides higher bending angle.The actuator consists of one side as extensible and the other side inextensible. Based on its anisotropic structure a stress is developed in the soft robot when it is pressurized or depressurized with fluid which results into the bending. An assumption is made for the soft robot to be of constant curvature type for modeling and sensing.

Figure 2: Fluidic soft robot used in the research

The important three areas of research related to soft robotics are material of the actuator, actuation methods and sensing [1]. One of the targets of this thesis is to select an appropriate curvature sensor for the soft robot.

1.1 Need of Sensor & Challenges in Sensing

In the traditional robots, there are fixed number of joints and DOF's ranging between 2 to 6 based on the robot type. The kinematics is defined by assigning links and frames on every joint and using certain mathematical methods to find the robots position and orientation or the joint angles. One of the most common approaches is using the **Denavitz Hatenburg** convention. Unlike this, the soft robots have large number of DOF. Additionally, the material used to manufacture the soft robot has a non-linear property. These reasons make it challenging to create an accurate model which can be used to determine robot state. However, there are other approaches to modeling which exploit the concept of Piecewise constant curvature used for continuum type of manipulators.

According to the literature, the continuum robot is made up of many sections which are linked serially and have many DOF's [20]. A specific case of this can be seen in Hannan and Walker describing the kinematic modeling for elephant trunk manipulator and which can also be used for other continuum manipulators [21]. The same theory can be applied to the soft robots. It is assumed that for a robot to be following the constant curvature concept it should have certain number of fixed curved links. The below **Figure 3** shows the overview of transformations in a piecewise constant curvature case.

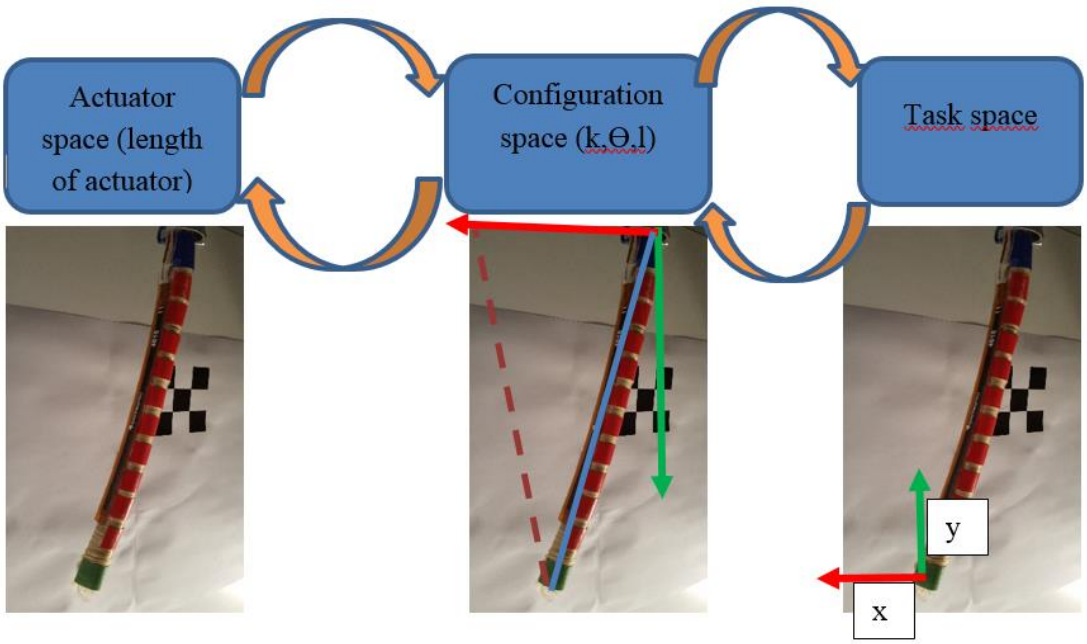

Figure 3: Kinematics in a constant curvature robot[20]

The actual length of the soft robot is used to determine the configuration parameters which are curvature k, bending angle Θ, length of the section l. 'r' is the radius of curvature. Then the configuration parameters are used to find the tip position as shown in below diagram.

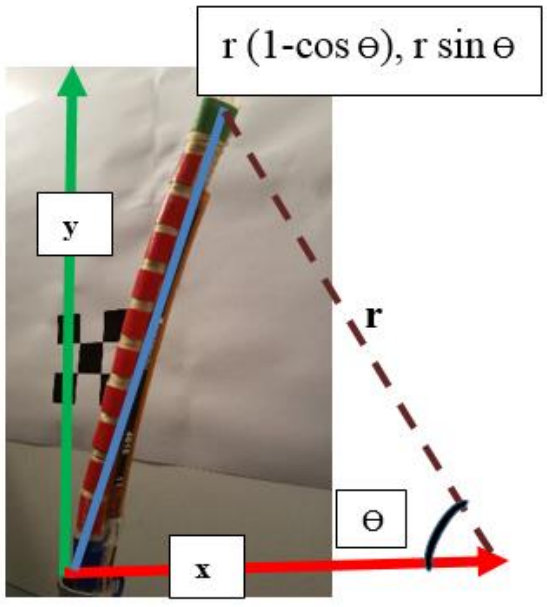

Figure 4: Finding tip position from arc parameters with PCC

Thus in the above case , the whole soft robot can be considered as 1 section and the sensor reading can be used to calculate curvature and the bending angle, which can be used to calculate the tip position[20]. There are some assumptions of this PCC concept, which are needed to be considered. In case the soft robot is of larger size, then the soft robot is should be discretized into many fixed curvature sections consisting of sensor on every section. This would give the overall bend of the soft robot more accurate.

There is an enormous research ongoing to develop appropriate soft sensor's that provide the necessary position, force and other information depending on the type of sensor. A challenging part of this is that the sensor should benefit the compliance feature of the soft robot and not add as an additional weight and stiffness. This requires study of sensors that are thin, flexible, soft and can be easily integrated to the soft robot, providing tip and force information. There has been development of sensors of above-mentioned characteristics with almost all of them assuming a constant curvature bending.

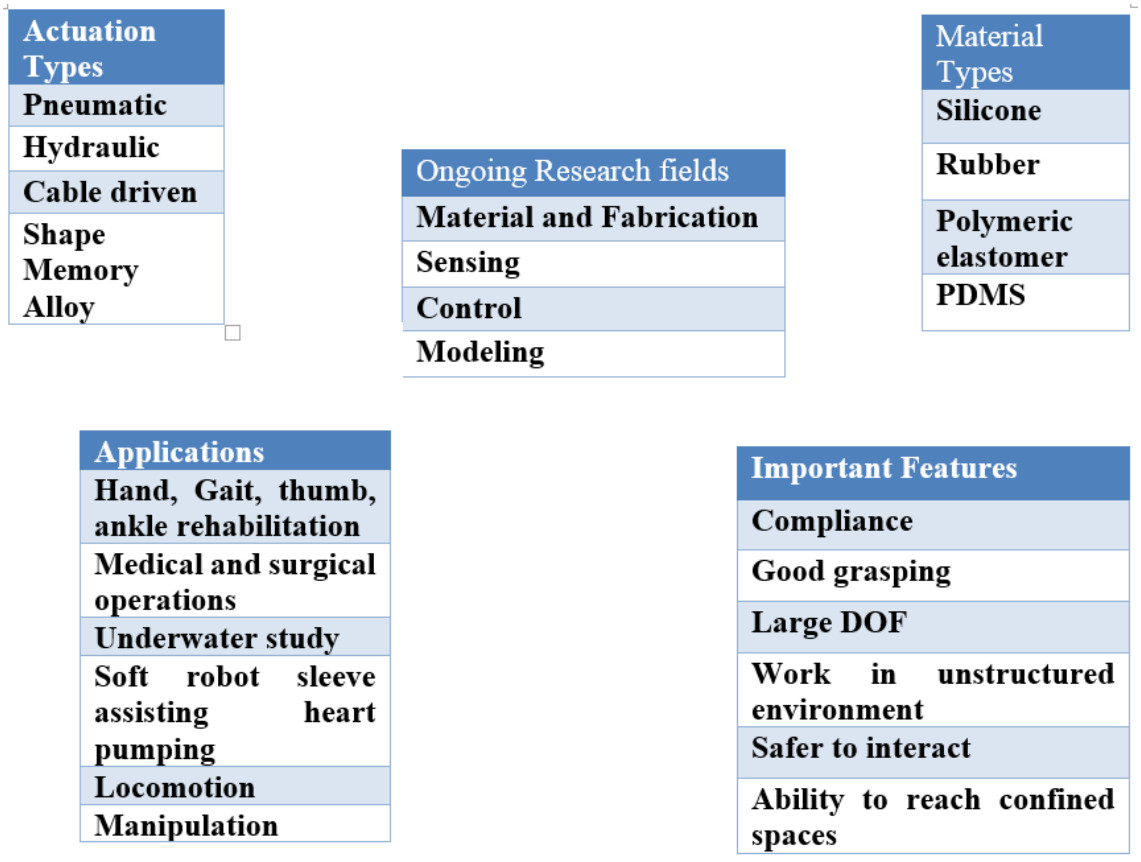

Figure 5: Summary of the soft robotics in general[21]

1.2 Research Objective

The huge number of degrees of freedom along with the material of the soft robot being non-linear , makes the modeling of the soft robot very challenging[1]. The modeling method inspired from continuum manipulators involves using the PCC concepts. The other approach is to use large number of curvature sensors on every small sections of the soft robot. Instead of adding large number of sensors and adding more complexity and weight, this thesis will address the problem of finding the state of soft robot by:

1. Literature review and finding a suitable curvature sensor for the studied fluidic soft robot
2. Perform experiments by introducing obstacles in the robot path and collect the pressure sensor, curvature sensor and vision system data to:
    a. Use the collected sensor data, to train a model that determines the soft robot state, with and without obstacle presence.

1.3 Methodology

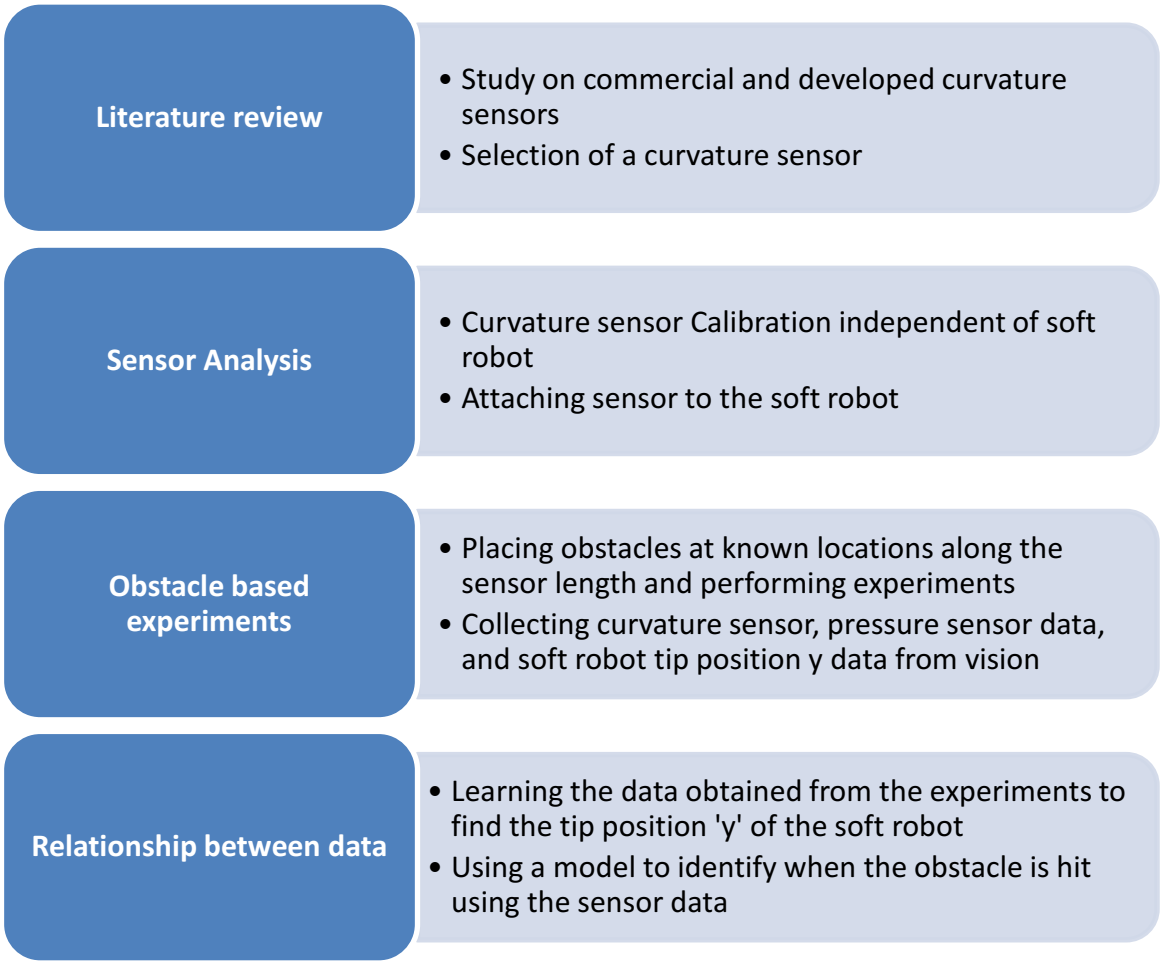

2 THEORETICAL BACKGROUND

Sensing choice demands a critical set of requirement solving phase especially in case of soft robotics. To find a promising solution the following literature review is done.

Optical sensing using FBG (Fiber Bragg Grating) [22] is a very accurate and repeatable method of providing bidirectional sensing as per [23] . The principle here is based on the reflected wavelength and relies on the assumption of *pure bending model*. Thus, a map of curvature vs reflected wavelength is obtained by this method [23]. Although the manufacturing is not complex it doesn't provide the sense of compactness due to the measurement setup hardware[24]. A disadvantage of FBG is a high temperature dependency as shown in [25]. Another optical method used consists of the sensor made up of a waveguide of stretchable polymer material and internally coated by a non-stretchable reflective material with led and photodiode as source of light and receptor respectively. Deformation including stretch, bend or pressure results into the formation of micro-cracks in the reflective material causing loss of light. This provides the map of curvature/strain/pressure vs light intensity(converted to voltage) [26]

Vision system can be used to obtain the tip coordinates of the soft robot as it offers a good accuracy in stationary applications**.** However, in mobile applications it is required to have an embedded sensor, which limits the use of vision system. The vision system still can be used as a ground truth (reference) for calibrating some other selected curvature sensor.

Conductive ink sensor is a type of sensor which is commercially available as well as can be manufactured. In this a conductive ink is printed on a polymer substrate for e.g. polyimide [27] . The principle is that the resistance increases as the sensor is either stretched or bent depending upon the ink and substrate. Suikkola et al. has discussed a single section *stretchable sensor* made up of ***silver ink printed on polyurethane*** substrate which was used as a strain measuring sensor and tested for a stretchable RFID tag [28] This sensor is fabricated using screen printing technique and will be tested in this thesis.

The commercial option for this are ***Flex sensor*** from **SpectraSymbol**[29] and ***Bend sensor*** from **Flexpoint** [30]. Both the Flex and Bend sensor work on the same principle of increase in resistance as the sensor is **bent**, but are produced by different manufacturers. Bend sensor has more features in a sense that it can measure bidirectional bending, and has variety of laminate and substrate options. Flex sensor is robust, cheap and has a linear measurement output. But, it suffers from large hysteresis [31]. A comparison study in [32]proves bend sensor to be a repeatable and low hysteresis providing sensor. Moreover, it shows how only a bare sensor gives repeatable readings whereas the laminations provided for protection add to large decays in the measurement values. Another study with the bend sensor is where the bend sensor is embedded inside

a pneumatically actuated 3D printed soft gripper to identify the grasped objects [7] . Due to commercial availability and ease of attachment, it is considered to test both these sensors.

Jamie Paik et al. compares Conductive ink sensors discussed above and ***Conductive polymer composite sensors (CSC)***. Conductive Polymer sensor's work on the same principle but they are manufactured by depositing conductive ink on rubber [33][34]. The results deduced through recoverable drift, transient response, and quasi-static response suggested Conductive ink polymers to be better than CSC sensors [35]. Additionally, the results observed that the harder polymer or base substrate for conductive ink polymers enables the conductive ink to regain its original position due to their higher elastic forces providing low hysteresis.

Electro conductive yarn is one of the sensor where the steel fibre is used with certain material property, which causes the resistance to change as the fibre bends or elongates. Three electro conductive yarns are used here to calculate the tip pose of a pneumatically actuated soft robot[36] . This is a good candidate but challenging to embed in the studied fluidic soft robot. One possibility can be to attach the yarn around the fluidic robot and see the results.

Two ***IMU sensor's*** (reference at the base and other at tip) are used by Mahdi et al for hand rehabilitation in a soft and rigid actuator which measures the angular velocity of fingertips which is then used after processing to determine the trajectory of finger tips [37]. This is a good sensor for hybrid applications but for soft robot, the signal conditioning circuitry and the IMU sensor itself can prove bulky.

Further, Amir et al. proposed stretchable sensor made with ***meshed pattern of metal*** on constantan polyimide laminate, providing strain results as resistance changes [38]. A maximum stretch of 20% is observed for this sensor. This also requires a careful manufacturing process with care to be taken to avoid problems of over-etching and unreliable sensor readings which can be a result of not removing metal parts in bare areas.[38]

The most interesting sensors discussed are the ***liquid metal-based strain sensors*** [39][40]. Among choices of different liquid metals, *EGain* prove to provide better results [40]. They have good accuracy, repeatable and linear characteristics. However, a very complicated manufacturing process due to the injection of liquid conductor into the channels[41][8]. The problems related to fabrication can be overcome by the methods described by [42] involving ***Mask deposition of the liquid metal***. Additionally [43] describes a fabrication method wherein a 3D printer is specially built to directly print the resistive carbon ink in the reservoir.

There are other similar sensors like hydrogel and liquid carbon black sensors but the former suffers drift issues due to drying and in the later also the liquid carbon dries and

has to be replaced [44] [45] .

Magnetic hall sensors for measuring curvature were also studied[46][47]. This proved to have good accuracy and linearity, with filtering required to eliminate noise. They are made up of a circuit of hall element and permanent magnet on flexible sheet, which produces a change in voltage with the change in distance between hall element and magnet. In order to use this sensor for measuring the curvature of the whole actuator a sensor of arrays is required.

The below Table gives overview of the sensors discussed.

Sensor name	**Type**	**Repeatability**	**Hysteresis**	**Manufacturing method**
EGain	Stretch	Good	High	Complex 3D printing
Hydrogel	Stretch	-	-	-
IMU	-	Good	-	-
Electroconductive yarn	Bend/Elongation	83%	47%	Complex to embed
Optical sensor				
a)Led photodiode	Bend	reasonable	Hysteresis present at 4 mm/s	Easy
b) Bidirectional FBG	Bend	High	_	Standard FBG embedded in silicone rubber-3D printing
Magnetic sensor	Stretch	-	Less	Flexible electronics
Bend sensor	Bend	High	Low	Commercially available
Flex sensor	Bend	Low	High	Commercially available

Table 1: Comparison based on important sensor characteristics

From the literature it is observed that the type of sensor being bend or stretch is also important to know. The bending sensors can be attached only to the inextensible side and the stretch sensors to extensible side of the soft robot. As the grasping occurs on the inextensible side where the bend sensors are attached, it is important to attach them such that it doesn't interfere with the task.

A study on the Glove Projects with specifically Flex sensors is done to understand the possibility of its applications.

Project reference	**Application**	**Brief explanation**
[48]	Glove producing music	Data from flex sensor, tilt sensor and distance sensor to produce sound
[49]	Mimicking human hand	Using input from flex sensors on glove to control the robotic hand
[50]	Convert gestures by hand to speech for deaf people	Data from flex sensors, accelerometer, gyroscope and compass is processed by arduino and sent via Bluetooth to mobile which translates text into speech
[51]	Used for VR	The data from flex sensor is captured with National Instruments device to collect the values of flex sensor
[52]	Control a Remote Control car using glove	The data from flex sensor, force sensor, vibration sensor and gyroscope is used to control the RC car

Table 2: Glove projects with flex sensor

The literature review covers wide variety of sensors. The most important criteria/challenges observed from the review for the selection of the sensor include

- **application of the soft robot**
- **type of actuator used**
- **fabrication method of the sensor**
- **availability of the equipment to manufacture the sensor**
- **complexity added due to signal conditioning**
- **measurement hardware required to get the final output**
- **embedding the sensor**

Taking into account all the above factors, the flex sensor from Spectra Symbol; bend sensor from Flexpoint; and silver ink stretchable sensor are selected as suitable candidates for the fluidic soft robot.

The reason for selecting Flex and Bend sensor:

- Commercially available
- Simple voltage divider circuit for signal conditioning and getting final output

The reason for selecting silver ink sensor:

- Availability of manufacturing equipment
- Simple voltage divider circuit for signal conditioning and getting final output

3 CURVATURE SENSOR ANALYSIS

In this chapter, tests are performed with bend sensor from Flexpoint and silver ink stretchable sensor before finally confirming the choice of Flex sensor.

Further, the calibration is done for the selected curvature sensor, independently as well as after embedding it to the soft robot. The curvature sensor reading is mapped to pressure, position and bending angle of the soft robot.

3.1 Experimental Setup

Actuation Mechanism and Controller

The soft robot is actuated using a digital hydraulic drive system. The system comprises of a high pressure valve, a low pressure valve, reservoir system and storage tank. The medium of fluid used is water. The maximum pressure that can be provided by the system is 600kPa.

The hardware used for the soft robot's control is *dSPACE MicroAutoBox*. The working environment to perform operations on the hardware is provided by the ControlDesk software. The code for manipulating the soft robot is written in Matlab, which is linked to the HMI in ControlDesk. The output and ground wires from the curvature sensor and pressure sensor are connected to the input ports of the controller hardware. The communication is enabled via CAN. Hence, both the sensor readings can be measured and are visible on the ControlDesk HMI. The soft robot can be actuated manually by clicking the **PA** option to increase pressure by opening the high pressure valve, and **AT** to decrease the pressure by opening the low pressure valve. The robot can be actuated automatically by clicking the PWM option. Below **Figure 6** shows the ControlDesk interface.

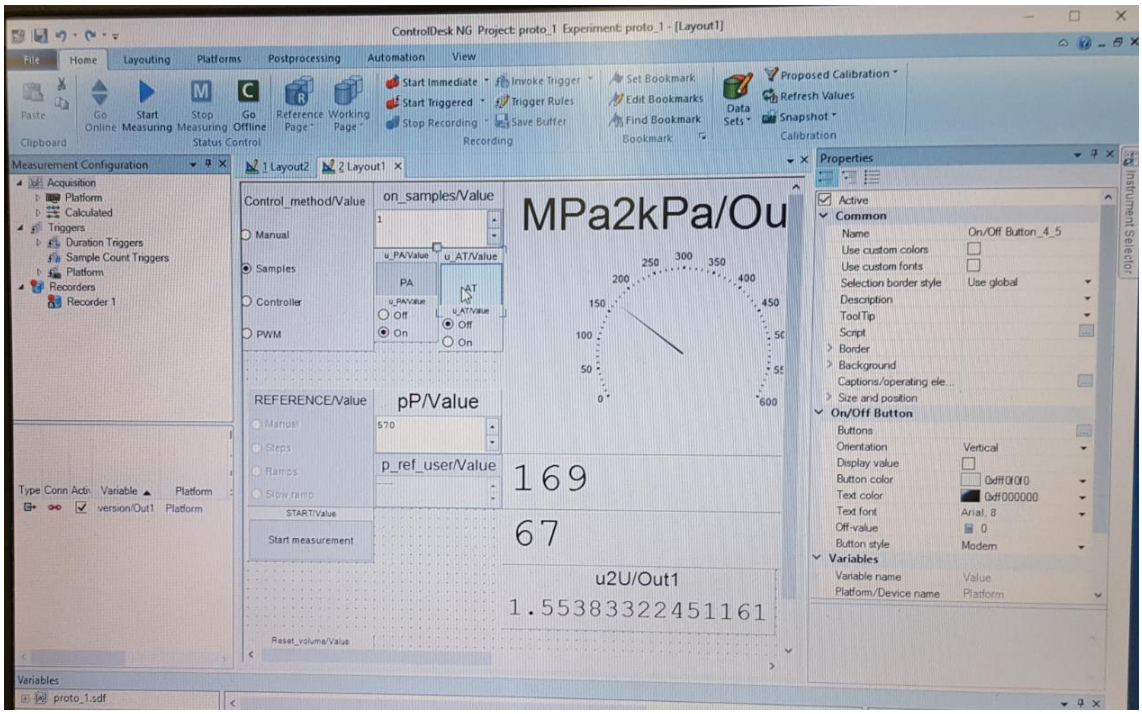

Figure 6: ControlDesk interface for controller

Vision system

The ground truth calibration for the curvature sensor is done using a vision system. The vision systems helps for calibration of a large range of angles. A Go-pro camera is used for this purpose. The camera is placed on a tripod and the area where the tripod is placed on the ground is marked, so that next time the tripod can be placed at the same spot ensuring repeatability of experiments. The camera is turned ON and OFF using the Go Pro app on mobile phone. The camera is connected to the app through Wi Fi. This is done to ensure no hindrance to the camera location. A blue and green marker is placed at the base and tip of the robot respectively, and red markers cover the entire length of the actuator. The GoPro camera records the motion of the robot when it is actuated. The recorded video is then post-processed using a Simulink model. This model fits a circle to the points identified by the red markers, to calculate the chord length and radius, and thus finds the bending angle of the actuator. The model also provides the tip position(x and y co-ordinates in the 2D plane) of the soft robot. The **Figure 7** below shows the robot with markers.

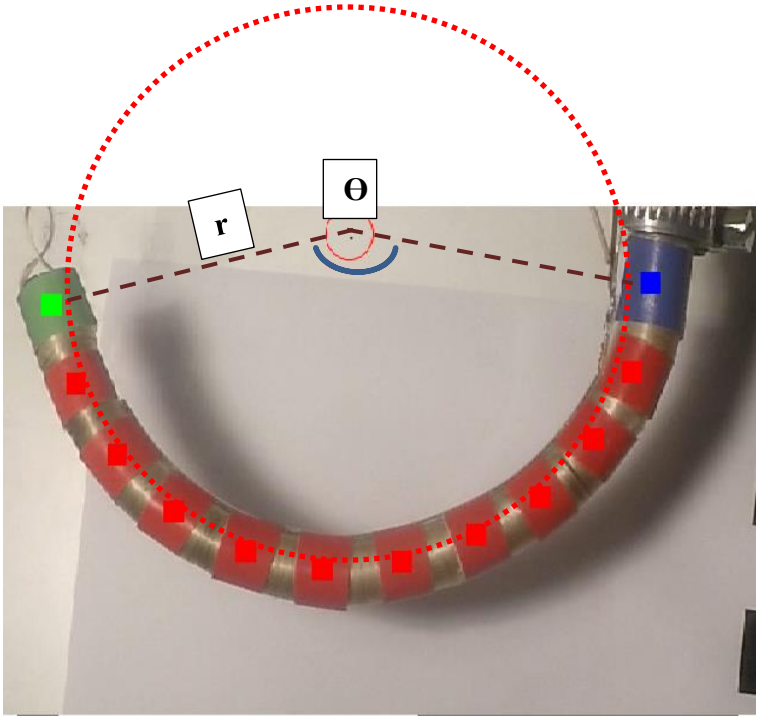

Figure 7: Calibration using the GoPro camera

3.2 Testing Flexpoint and Silver Ink curvature sensors

Two 3inches bidirectional un-laminated Flex point bend sensors were selected. The choice of bend sensor was due to its characteristics of having low hysteresis and repeatability as observed in [32] One of the sensors was attached near base and the other at the tip. The readings obtained from the sensor were not reliable. Sometimes both the sensors would give similar voltage readings but in other set of experiments completely different. The reason was due to the wires coming out from end of the tip sensor and continuing on top of the other as below **Figure 8.** Further, the base of this sensor was wide causing difficulty to stick to the soft robot surface. Thus, this sensor was discontinued.

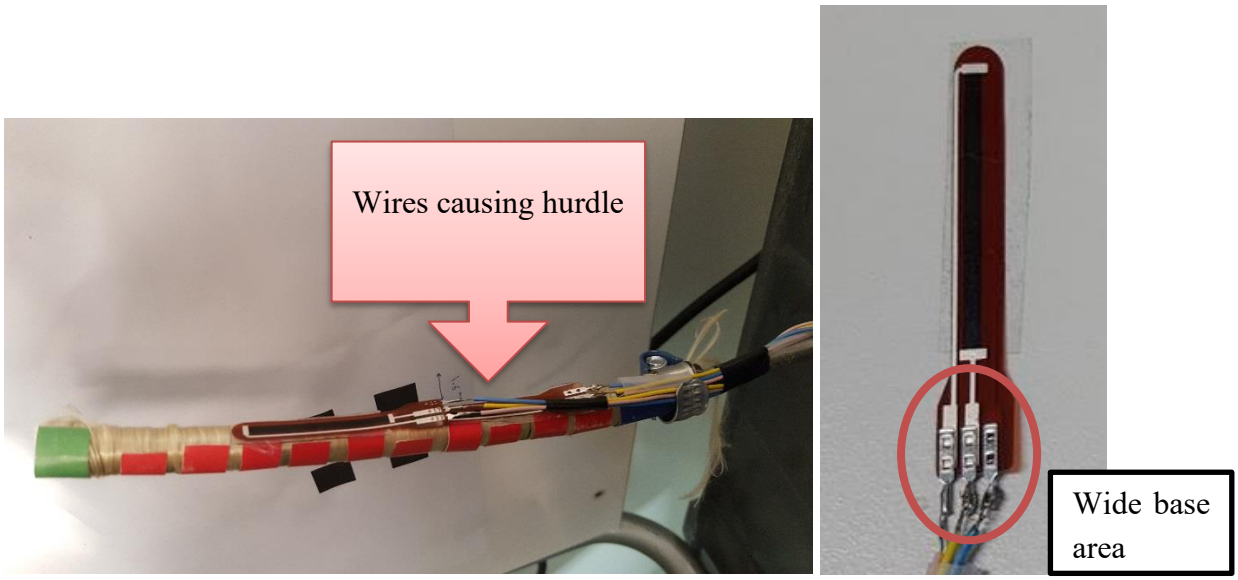

Figure 8:Flexpoint bend sensor attached to soft robot

The next sensor that was selected was the Silver ink stretchable sensor[28]. The principle of the silver ink stretchable sensor is that the resistance increases as the sensor is stretched. Hence, this sensor had to be attached to the extensible part. Attaching this sensor to the soft robot seemed very challenging. This was due to the polyurethane substrate of the sensor, which was very delicate. In order to provide useful readings the sensor should be wrinkle free. The windings of fibre on the soft robot and markers for camera calibration made it difficult to attach it appropriately. Moreover, the base of the sensor with the interface of the sensor to the wires was very fragile. The stretching of sensor created a tension at the interface. The sensor did not seem to show any appropriate results while testing. Thus, the use of the sensor was discarded.

One way to overcome this problem could have been attaching some substrate to the base to give it more strength. Further, this sensor can be easier to attach in the soft actuators like the PneuNets where the surface is plain and free of windings.

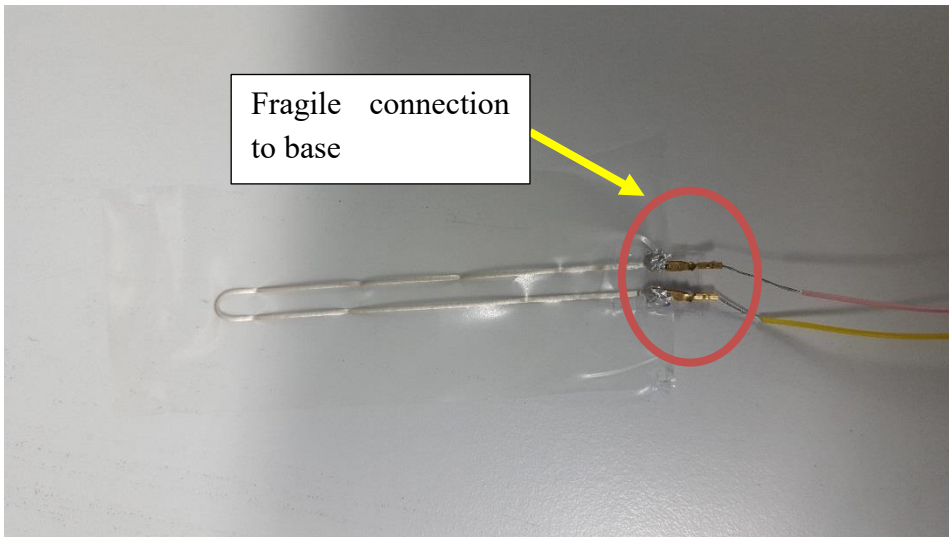

Figure 9:Silver ink stretchable sensor

The literature provided many sensor options. However, based on the studied fluidic fibre reinforced soft robot, the flex sensor proved to be a good choice because of following reasons:

1. Commercially available at a cheap price
2. The sensor doesn't have temperature dependency like FBG optical sensor
3. Thin and robust
4. Easy to embed compared to other sensors
5. Easy signal conditioning
6. Provides linear result

Throughout the thesis, the flex sensor will be termed as curvature sensor.

3.3 Construction and working of flex curvature sensor

The selected curvature sensor named as **flex sensor** is based on conductive ink coated on a plastic substrate from Spectra Symbol[29]. As the sensor is bent, the conductive particles inside shift further apart from each other, which causes the resistance to increase. The sensor length subtends a central angle, which is the bending angle. The formula used is, $s = r * theta$, where 's' is the length of the sensor which is constant(9.525cm), 'theta' the bending angle(central angle), and the radius of curvature is 'r'.

The sensor's flat resistance and fully bent resistance are observed using multimeter as 8.7kohms and 15 kohms respectively. The resistance is then converted to voltage using a simple voltage divider circuit. In order to obtain a good range of values, multiple values of static resistance like 12K, 15K, 18K, 22K, 47K are tried. The value of 10K proves to give appreciable range of readings.

3.4 Independent sensor calibration with 3D setup

The curvature sensor is calibrated using a 3D printed curvature setup as shown in **Figure 10** providing curvatures for angles corresponding to 30° - 90° as **0.05cm^{-1} to 0.165cm^{-1}** respectively**.** The calibration setup was 3D printed using a MakerBot printer. Arduino microcontroller Atmega 2560 is used to perform initial tests on sensor. A simple Arduino code gives the resistance and voltage values when the sensor is being placed on different curvatures of the setup. The aim of using 3D printed setup is to test the sensor solely. Later on the sensor is attached to the robot and again the 3D printed setup is used to repeat calibration on soft robot. The motive of using the 3D set up is to obtain a second verification to the vision system and consider the manufacturing effect of sensor.

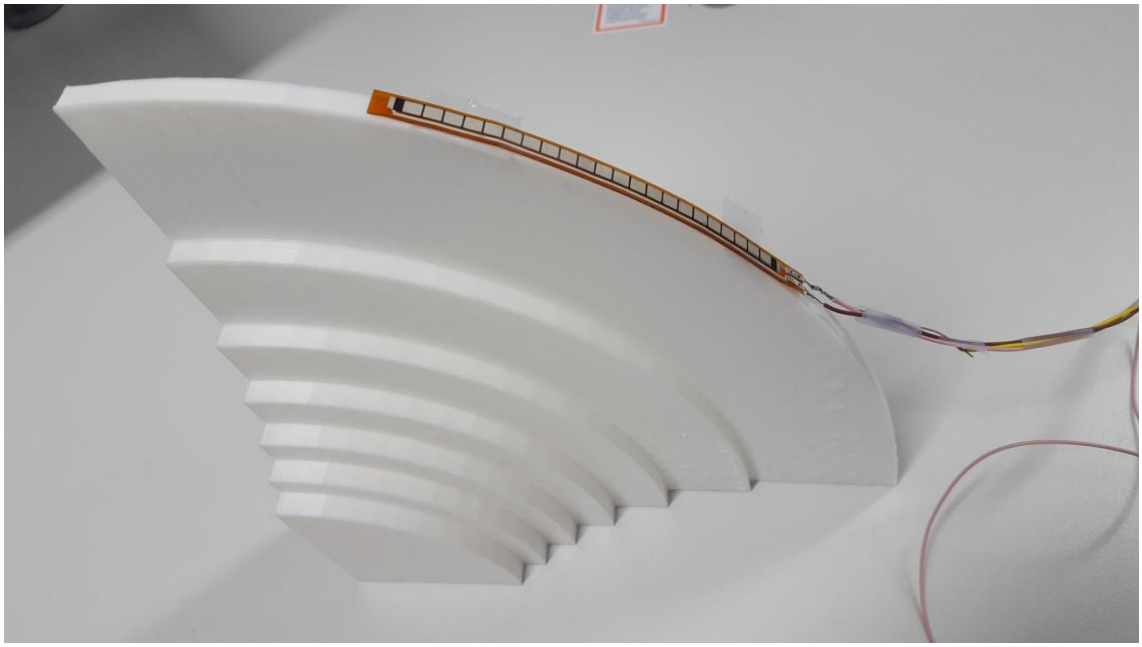

Figure 10: 3D printed setup for calibration

The curvature sensor reading vs Bending angle map is plotted in Matlab as shown in **Figure 11**. A linear function is obtained which is, $V = 0.007 * \Theta + 2.3$. Further sensor vs curvature is plotted which is, $= 3.8 * k + 2.3$.

Where, k is the curvature.

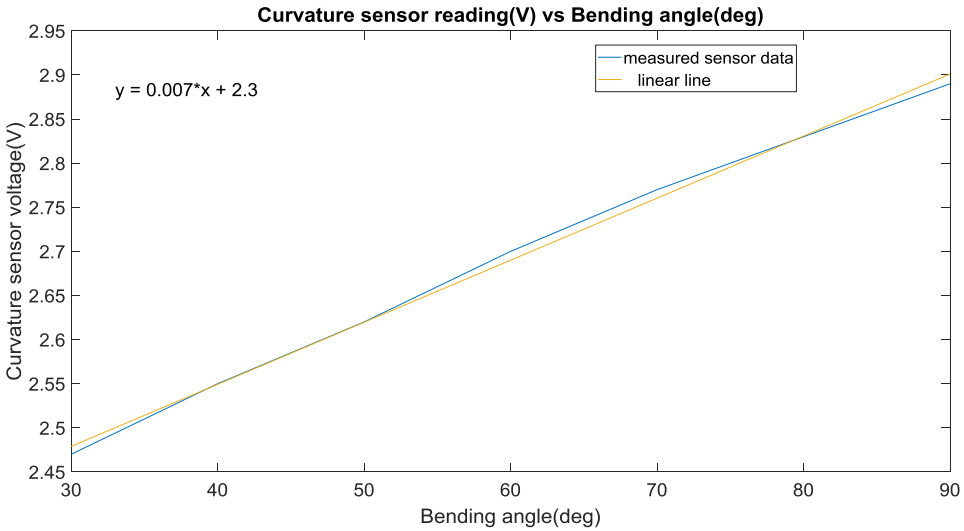

Figure 11: Bending angle Vs Sensor voltage map

3.5 Attaching sensor to soft robot

The next step is to attach the sensor to the soft robot. Attaching the sensor to the soft robot is challenging as the adhesive or the tape used to attach causes deviation in the true reading. For instance, the sensor was embedded fully inside the soft robot and a layer of rubber was coated around it. Although the sensor was providing some reading, the overall stiffness of the actuator increased and it did not provide the required bending. The below figures show the maximum bending which is very less.

Figure 12: Describing the low bending due to embedding sensor completely inside the robot and coating it with rubber

Figure 13: Failed method to attach sensor as wounding the tape caused difficulty in appropriate sensor bending

Figure 14: Correct attachment method for sensor

After certain trials with different tapes, the sensor is attached using a silicon double-sided tape to the inextensible side of the soft robot. Care is taken, such that the base of the sensor is appropriately attached, so that it should not break after multiple runs.

The soft robot is now actuated to 400kPa. The dspace controller records the curvature sensor reading and the internal pressure of the soft robot.

The 3D setup is used again to verify if the sensor gives the same reading as earlier. The soft robot is actuated using the PA (increasing pressure) option until it bends according to the shape of the curvature on the 3D setup. This is done for all the curvatures of the setup. The results obtained were similar as compared to independent sensor readings confirming the attachment of sensor as appropriate.

One of the challenges here was to synchronize the tip coordinate data obtained from the Go Pro camera. The reason is because; the Pressure and curvature sensor readings are collected from dspace, which is independent from the Simulink model, which processes GoPro video. Following steps were carried out to ensure proper collection of data:

1. Connect the GoPro camera to the mobile app
2. Press the recording option on ControlDesk HMI (recording measurement data i.e. curvature sensor and pressure sensor) and camera via mobile phone at the same time.
3. Then enter the S.P. for pressure at 400kPa

The below table summarizes this experiment:

Sensor used	**Measured parameter**	**Units**
Curvature sensor	Raw sensor data	Volt
Vision system	Soft robot tip y, Bending Angle	mm, degree

Table 3: Summary of sensor and measured parameters

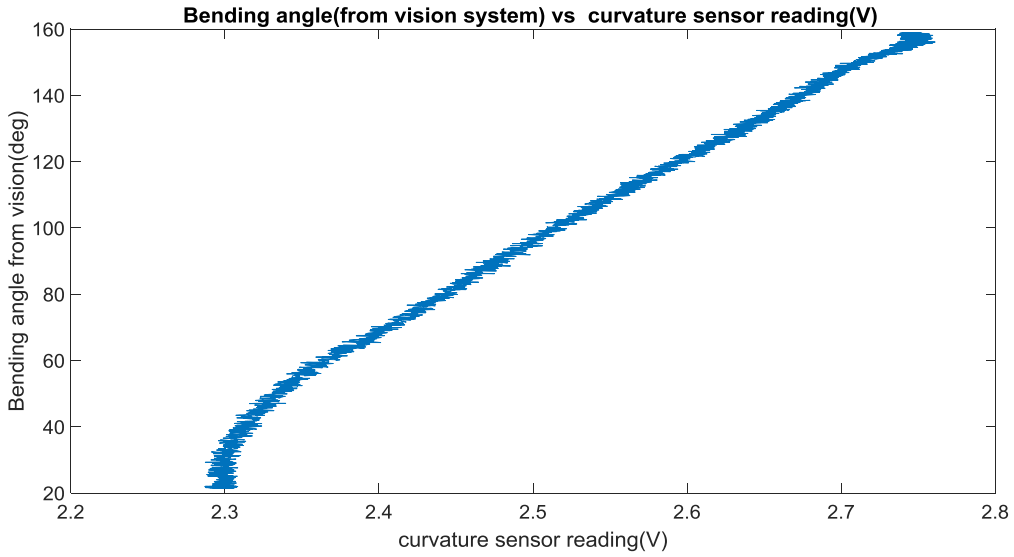

Figure 15: Map of Bending angle from vision (deg) vs curvature sensor reading (V)

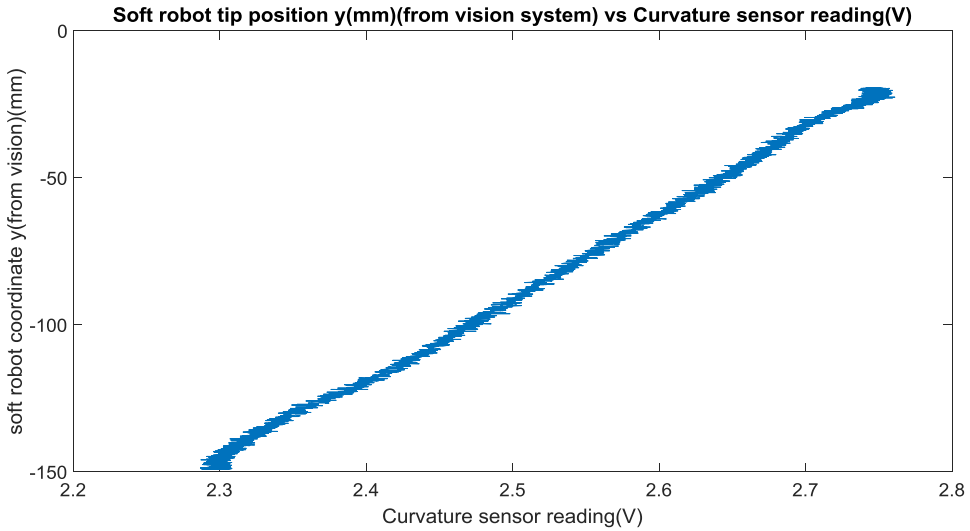

Figure 16: Map of soft robot tip position y(mm) vs curvature sensor reading (V)

The Bending angle vs curvature sensor reading and tip coordinate y of soft robot vs curvature sensor reading is been mapped completing the calibration of the soft robot. In this way, it is seen that the curvature sensor can be used giving information about how much the robot is bent via the bending angles and the tip of the position of the soft robot. This information can be used for appropriate control of the soft robot.

However, the above information is valid only when the soft robot moves freely in environment without the presence of any obstructions. Chapter 4 and 5 will describe how the pressure and curvature sensor can detect the obstruction occurrence.

4 EXPERIMENTING EFFECT OF OBSTACLE ON PRESSURE vs CURVATURE SENSOR READING

In this chapter, a number of experiments are performed by introducing obstacles in the path of the soft robot movement. The aim of this is to see how the curvature sensors' readings and internal pressure of the soft robot is affected when an obstacle appears along its path. The idea is to determine if the pressure sensor and the curvature sensor is able to detect the obstacle hit. Due to the obstacles coming in the way, the soft robot will not follow the ideal constant curvature path and will instead exhibit variable curvature. This chapter will highlight on what is the trend of the change in sensor readings depending on obstacle location. This would build the idea for the next chapter to model the trend of change in the different sensors behavior to obstacle location.

4.1 Experimental setup

The setup comprises of the soft robot attached with the curvature sensor on its inextensible part as in the previous sensor study. The obstacle is selected as a screw. Holes are drilled at different locations on a white board, which is hung behind the soft robot. The hole/obstacle locations are named as **base**, **mid**, **tip** with **base** location being the closest to the base of the soft robot and **tip** towards the tip of the robot and the end of the curvature sensor. A screw is fitted every time inside the hole locations, **base to tip** and its effect on the different sensors used in this experiment are noted. The obstacles are placed along the length of the curvature sensor and not after the sensor ends. The **Figure 17** below shows the experimental setup.

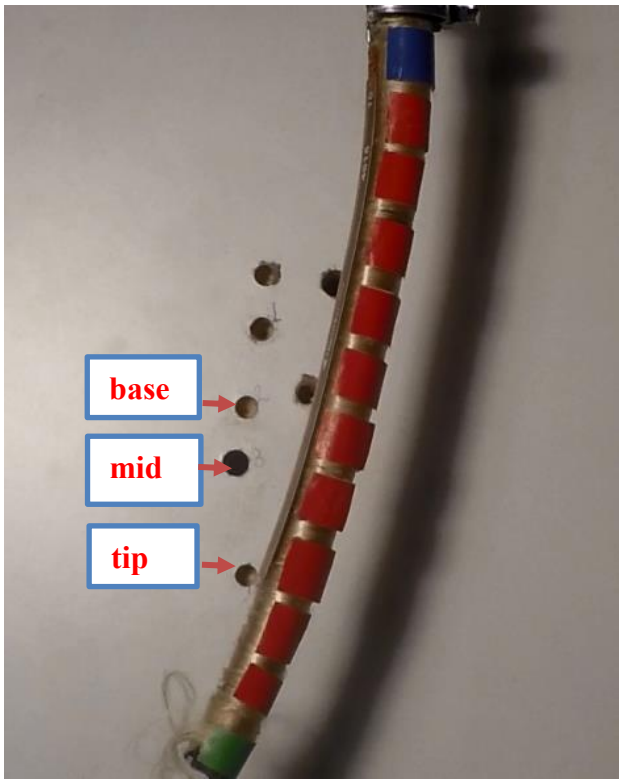

Figure 17: Soft robot with the obstacle locations

Obstacle name	Obstacle y coordinate(mm)
Base	-75
Mid	-88
Tip	-110

Table 4: Obstacle location y coordinate

4.2 Preliminary tests

Initially some short preliminary tests are performed without the obstacle. The aim is to control the curvature sensor reading. Hence, the curvature sensor reading is the controlled variable and the fluidic pressure which bends the soft robot is the manipulated variable. The Set point for curvature sensor is set at 2.596V for the first experiment and 2.730V for the second. After the first Set point is entered through the ControlDesk interface, the fluidic pressure keeps on increasing until the desired S.P. of the curvature sensor voltage is reached. The value of the pressure at which the desired S.P. is achieved is noted down. The soft robot is then de actuated and the same experiment is repeated for the second S.P. reading of the curvature sensor.

After this, a screw is fit into one of the obstacle locations. The same previous experiments controlling the curvature sensor voltage with the two S.P. values are repeated and the values of fluidic pressure to reach this S.P.'s now in the presence of obstacle are recorded.

Table 5 shows the pressure required to reach both these desired values of the curvature sensor for '**Free'** and '**Obstacle'** cases.

Curvature sensor reading(V)	Pressure(kPa) **FREE CASE**	Pressure(kPa) **OBSTACLE CASE**
2.596	**350**	**400**
2.730	**450**	**568**

Table 5: Preliminary test for voltage and pressure in free and obstacle case

The comparison of both the cases show that the internal pressure of the soft robot is increased due to the introduction of the obstacle. Thus, explaining that a higher pressure is required to reach the same curvature sensor reading when there is an obstacle along the path of soft robot. This gives an idea that the pressure and curvature sensor would produce a visible change on encountering obstacle.

In all of the experiments performed below, the soft robot is made to reach a desired S.P. pressure of 400kPa. This is enabled using a pressure feedback. The reason to keep the same pressure is to obtain a benchmark to compare the soft robot bending in free case and bending in obstacle scenarios. Another reason is to see what happens to the pressure at the instant the obstacle is hit.

4.3 Sensor Mappings for Obstacle free case

Initially, the soft robot is actuated freely without the presence of an obstacle, and the internal pressure and the curvature sensor reading is recorded.

The below graph shows the curvature sensor vs pressure relation when actuated freely.

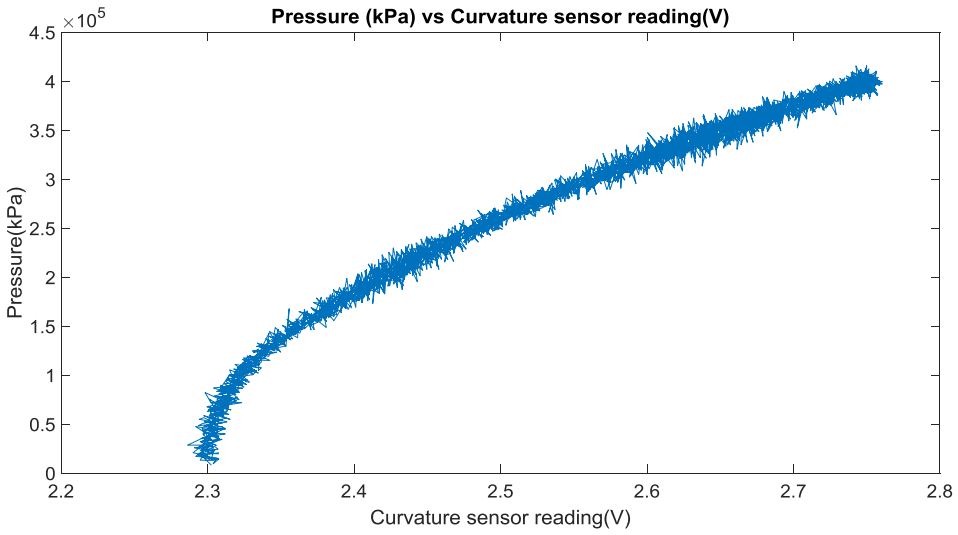

Figure 18: Pressure(kPa) vs Curvature sensor reading(V)

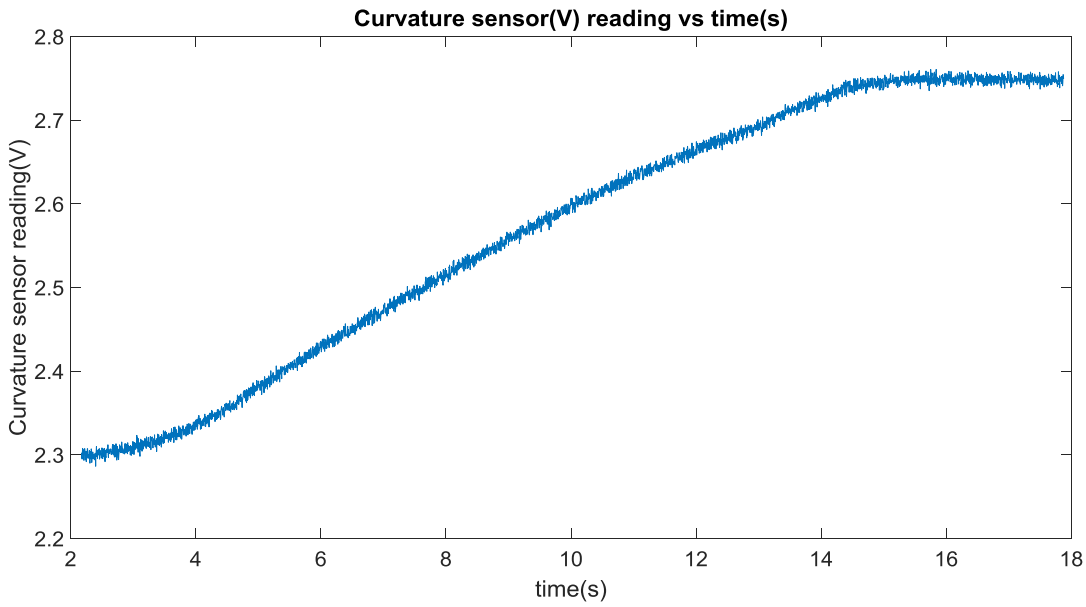

Figure 19: Curvature sensor reading vs time in free case

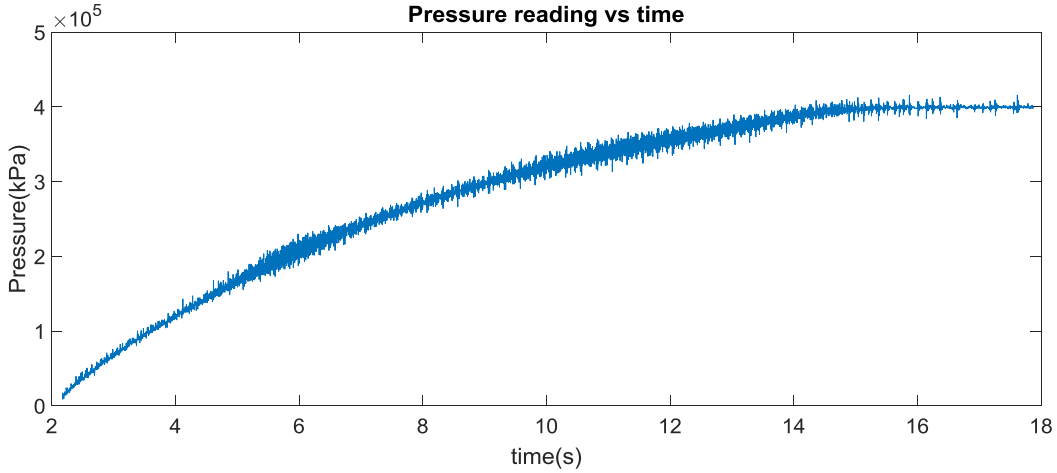

Figure 20: Pressure vs time

The readings are very noisy. Both the individual graphs of pressure vs time and curvature sensor time show the presence of noise in both sensors. Further, the noise is also due to the vibrations in the soft robot while it tries to reach the Set Point pressure of 400kPa.

4.4 Sensor Mappings in presence of Obstacles

In this step, the obstacles are introduced one by one starting from **base** location on the white board until the **tip**. The soft robot is then actuated and maintained at the desired pressure of 400kPa similar to the free case experiment. At the beginning of every experiment, the soft robot is fully de-actuated. The below **Figures** 21, 22, 23 describe the bending of the soft robot with all the obstacle cases.

Constant Data	Recorded Data	Experiments
Pressure_- 400kPa	Curvature sensor, pressure sensor, soft robot tip 'y' from vision system	Free case Base, Mid, Tip obstacle cases

Table 6: Summary of experiment

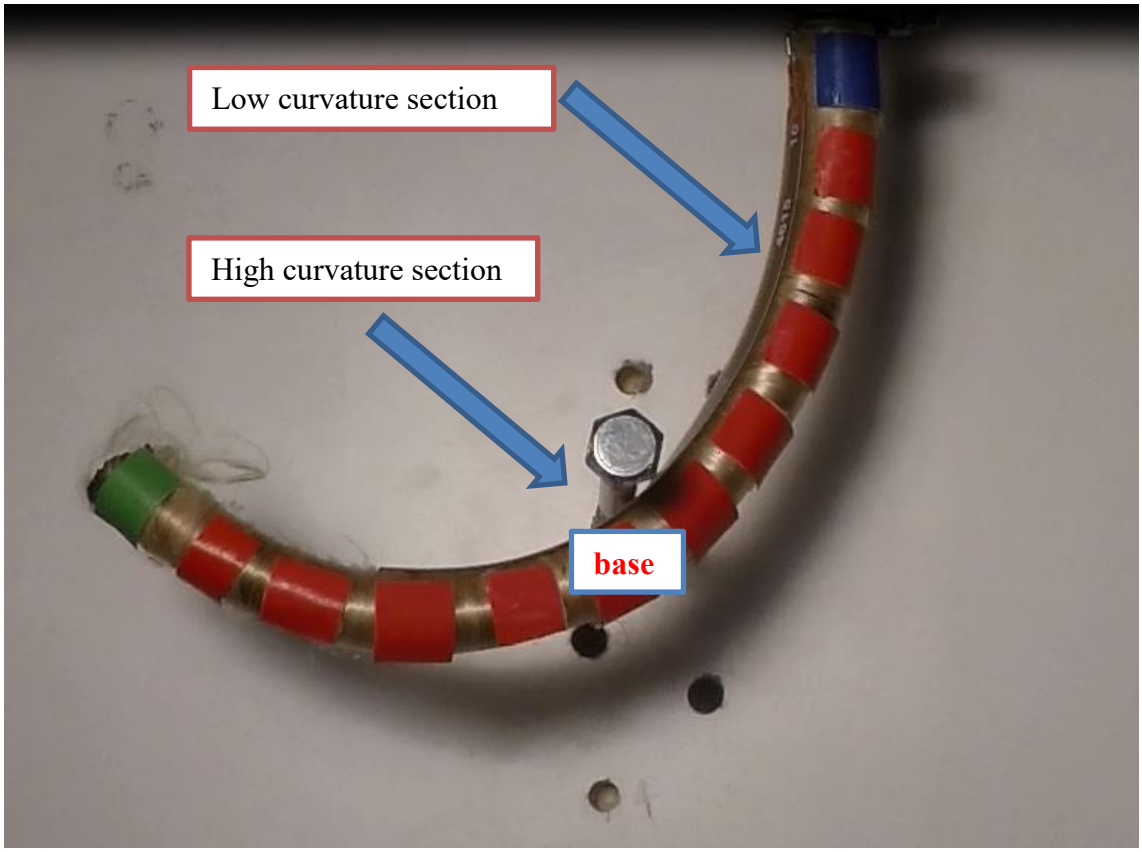

Figure 21: Soft robot in presence of base obstacle

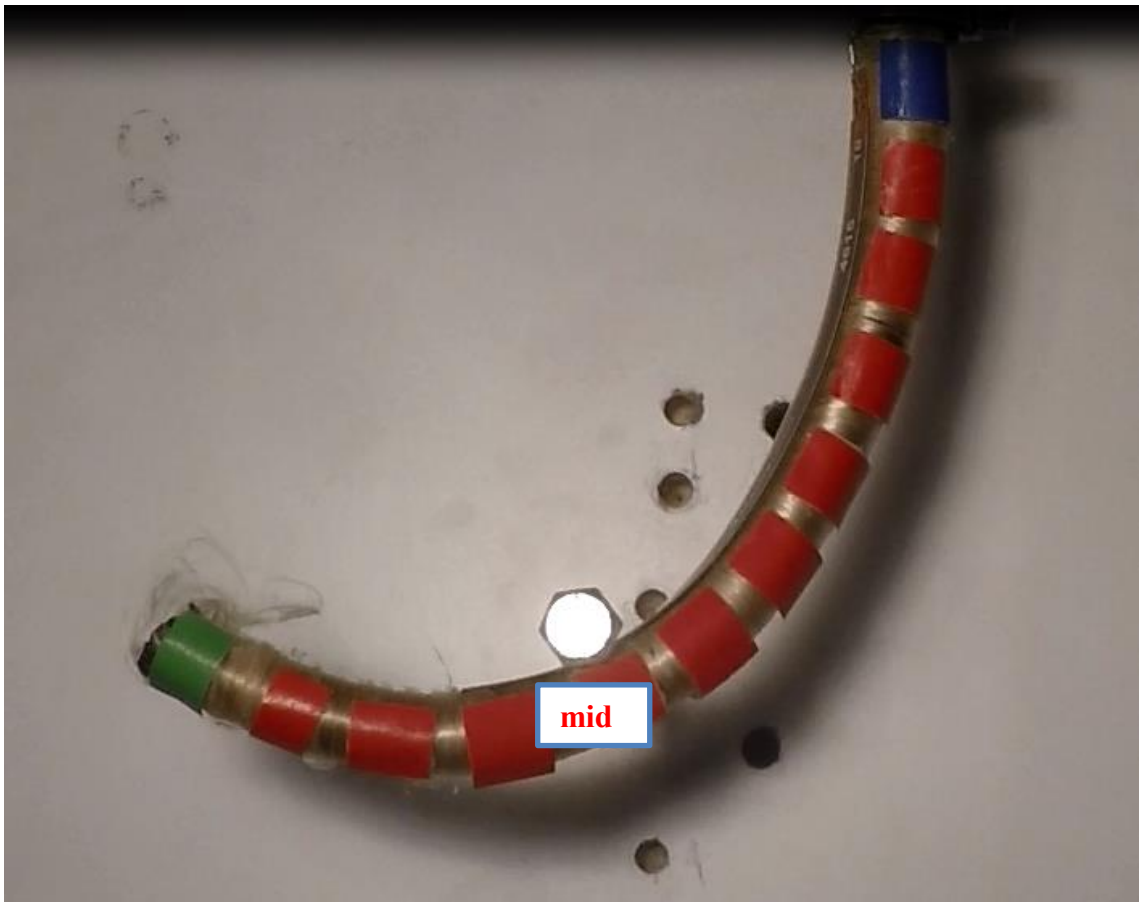

Figure 22: Soft robot in presence of mid obstacle

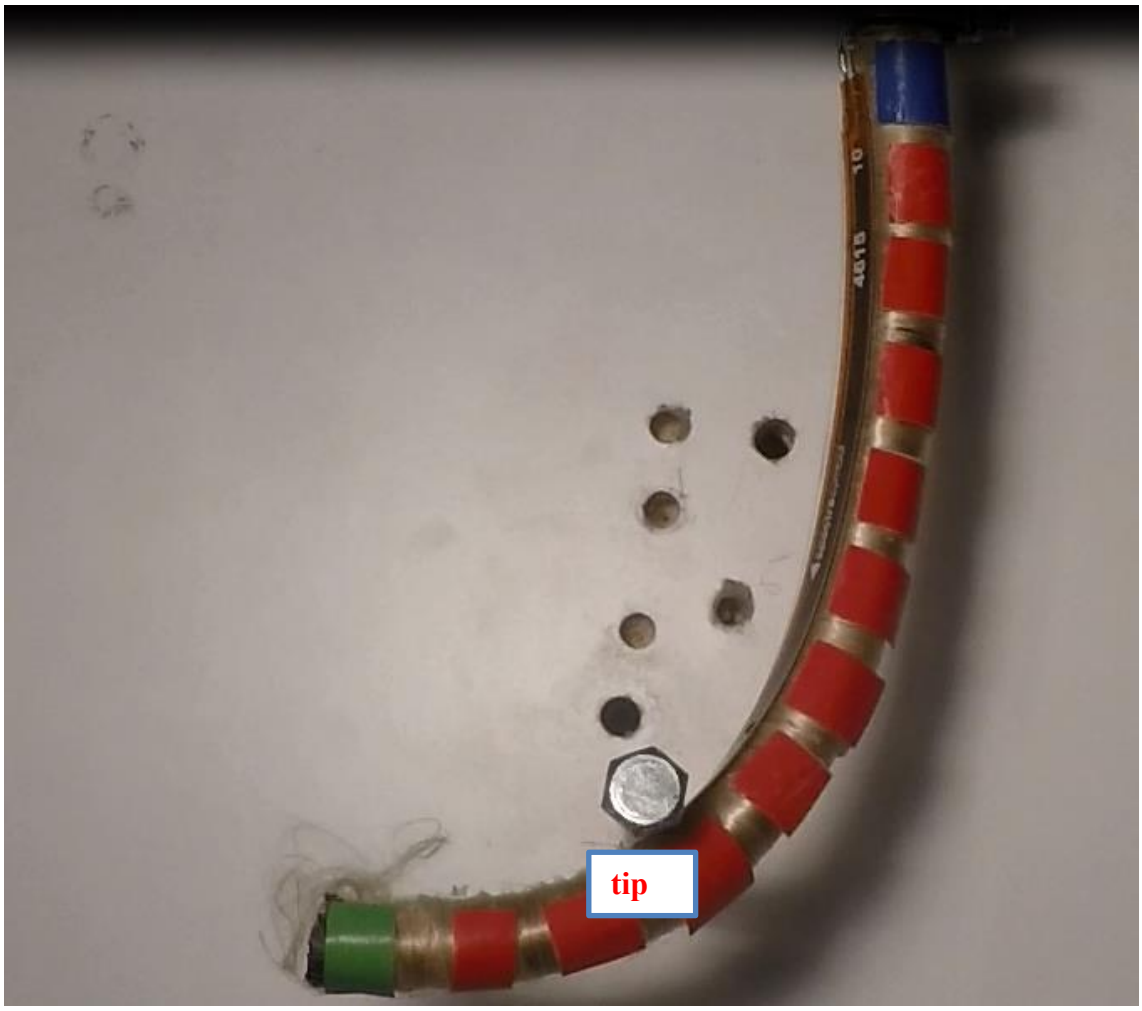

Figure 23: Soft robot in the presence of tip obstacle

When the obstacle is hit, the soft robot no longer bends uniformly or in a constant curvature shape. The curvature is higher at the point of contact of the obstacle, whereas the other part of soft robot has less curvature. In this scenario the soft robot no longer complies with the piecewise constant curvature theory. Thus, the comparison with free case as shown in **Figure 24, 25, 26, 27** shows the instance at which the obstacle is hit.

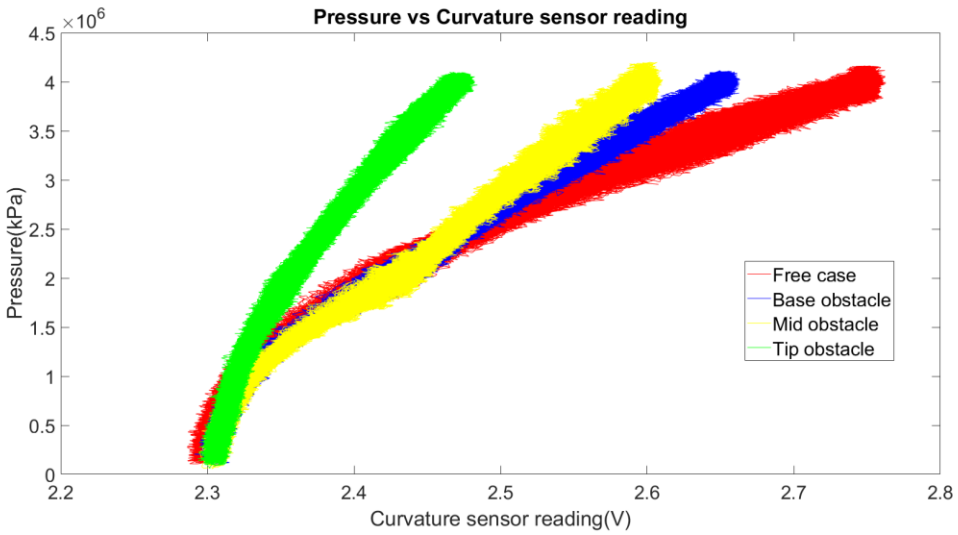

Figure 24: Pressure (kPa) inside soft robot vs Curvature sensor reading (V)

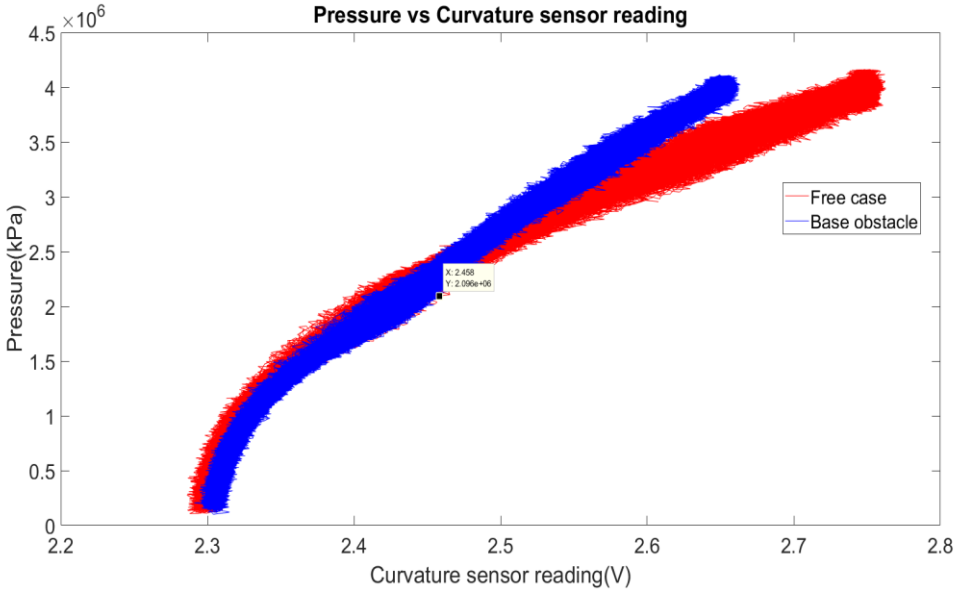

Figure 25: Deviation of base obstacle sensor values w.r.t free case

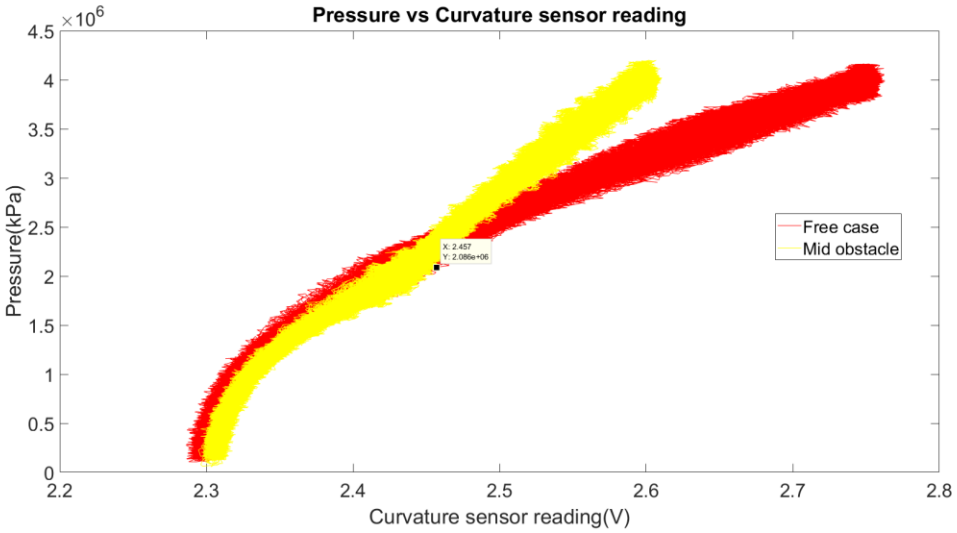

Figure 26:Deviation of mid obstacle sensor values w.r.t free case

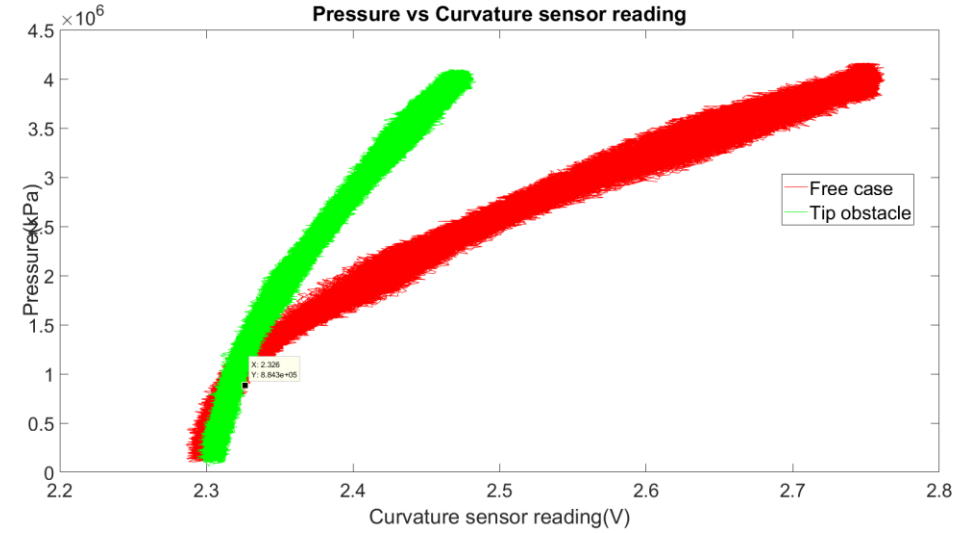

Figure 27:Deviation of tip obstacle sensor values w.r.t free case

The graph for base and mid deviates from the free case at 208kPa, and for tip at 88kPa. The base and mid follow almost similar trend as the obstacle locations are closer to each other. Moreover, the curvature sensor is unable to reach to the voltage as in free case. There is a decrease in curvature sensor reading as the obstacle location moves towards the tip of the curvature sensor. Again, this is because the section of the soft robot below which the obstacle is hit, has more curvature and the section above has low curvature. Hence, the overall curvature is reduced compared to free case.

Constant Data	Recorded Data	Experiments
Pressure_- 400kPa	Curvature sensor, pressure sensor	Free case Base, Mid, Tip obstacle cases

	Pressure KPa	Curvature sensor reading(V) at 400kPa	Pressure at deviation (kPa)	Curvature sensor reading at deviation(V)
FREE	400	2.762	-	-
BASE	400	2.661	208	2.457
MID	400	2.606	208	2.455
TIP	400	2.478	88	2.326

Table 7: Important observations from experiments

If the obstacle hits the soft robot at location y=-75mm (base); it will follow the trend shown in graph in **Figure 25**, for location y=-88mm (mid) it follows the trend in **Figure 26;** for location y=-110mm (tip) it follows the trend in **Figure 27**

It is clear from the experiments that it is possible to detect the obstacle hitting in a soft robot with the help of pressure sensor and curvature sensor. To benefit from this, the next chapter describes a model to learn these trends and predict the obstacle.

5 MAPPING AND CLASSIFYING SENSOR DATA BASED ON OBSTACLES WITH MACHINE LEARNING

The experiments performed in the previous chapter showed that the pressure and curvature sensor values change in a certain way after the soft robot encounters the obstacle.

In this chapter, the sensor values collected previously are learnt using existing Machine learning algorithms to determine the obstacle detection through two ways.

1. To predict the soft robot tip position y, given the curvature and pressure sensor values for all obstacle cases
2. To predict which obstacle location is hit given the curvature and pressure sensor values for all obstacle cases

The limitations and possibilities utilizing these algorithms in order to reliably predict obstacle detection is discussed.

5.1 Mapping curvature and pressure sensor to robot tip y

It is expected to use an algorithm, that is able to learn the trend that is followed by the soft robot tip y, whenever any obstacle is encountered in its path. For this, a Neural Network tool (nntool) in Matlab is used. The input data, target data and test input data are imported into the Neural network data manager. The **curvature and pressure sensor readings** are treated as **input data** comprising of **15076** observations, including the three obstacle locations cases and free case (tip, mid, base, free). The **y coordinate of the soft robot tip position** obtained from the vision system is treated as the **target data**. The below **Figure 28** describes the dataset.

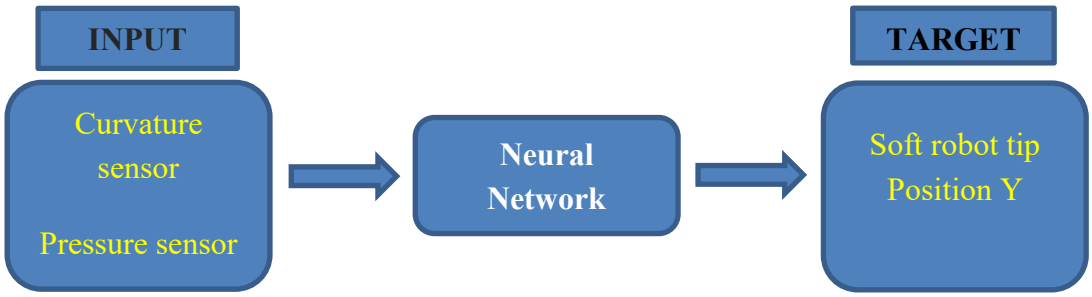

Figure 28: Description of data given to neural network

Neural network type	Feed-forward backpropagation
Training function	Levenberg-Marquadt backpropagation
Number of neurons	12

Table 8: Neural network properties selected

The above **Table 8** describes the necessary Network properties which are chosen. This results into a creation of network model as below which is trained with the dataset.

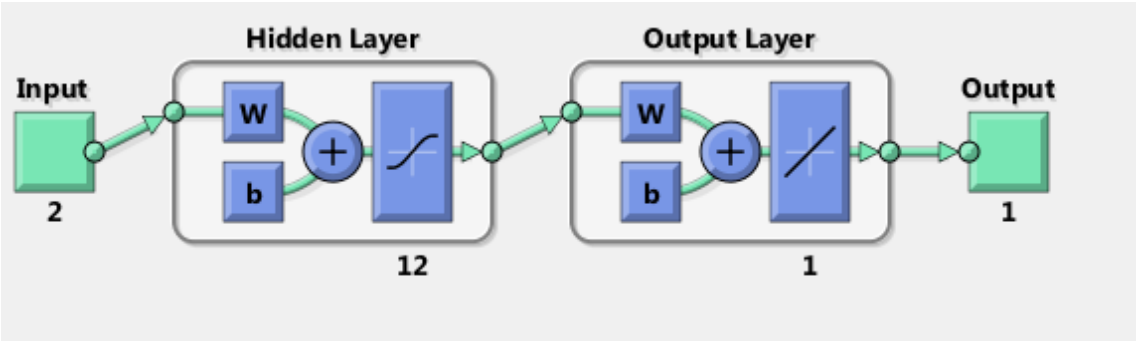

Figure 29: View of the created network model

Next, all of the 4 test cases consisting of curvature sensor and pressure sensor reading for base, mid , tip , free are given one after another to the trained model. Below graphs are the results obtained.

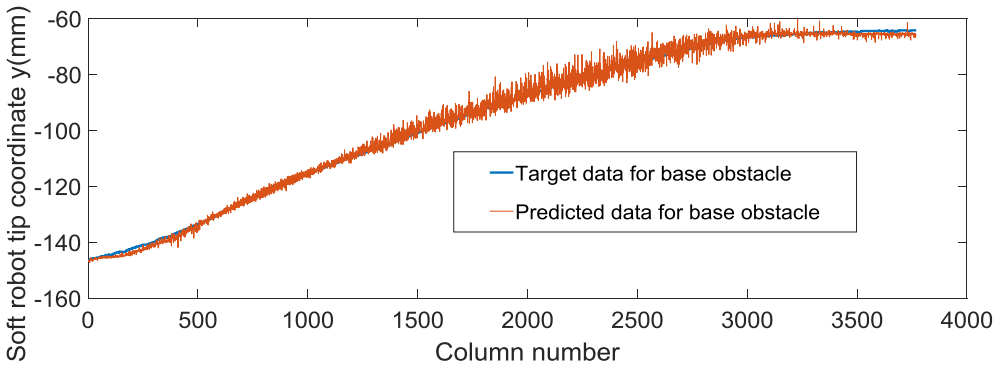

Figure 30: Target data for base obstacle vs Predicted data obtained

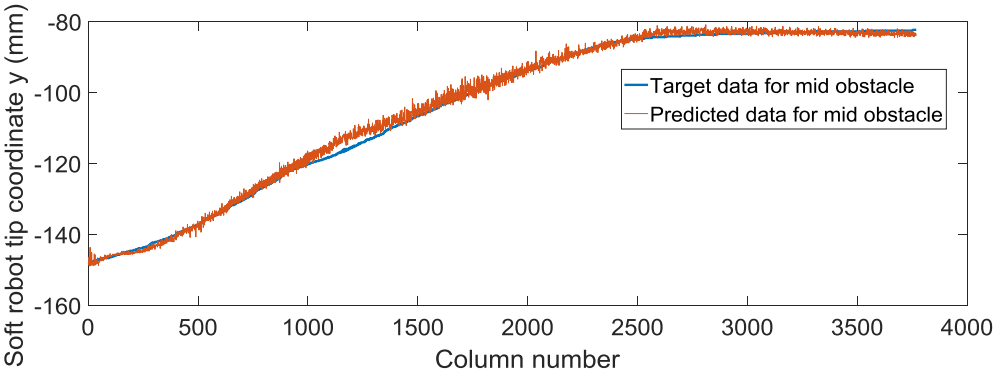

Figure 31: Target data for mid obstacle vs Predicted data obtained

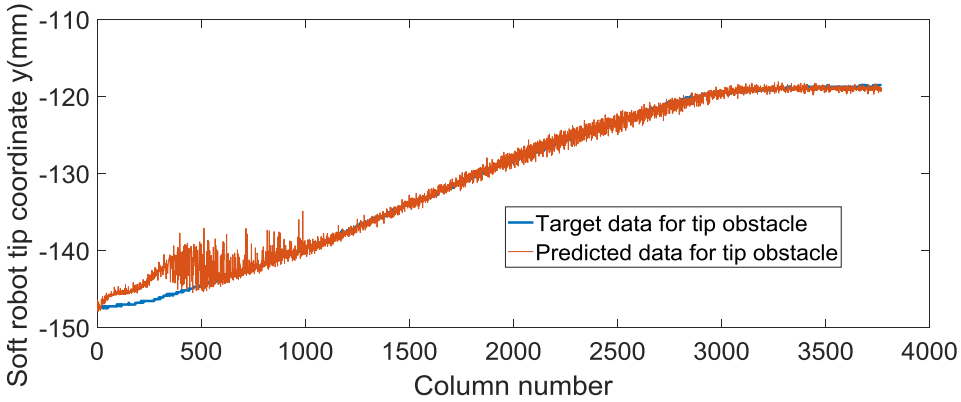

Figure 32: Target data for tip obstacle vs Predicted data obtained

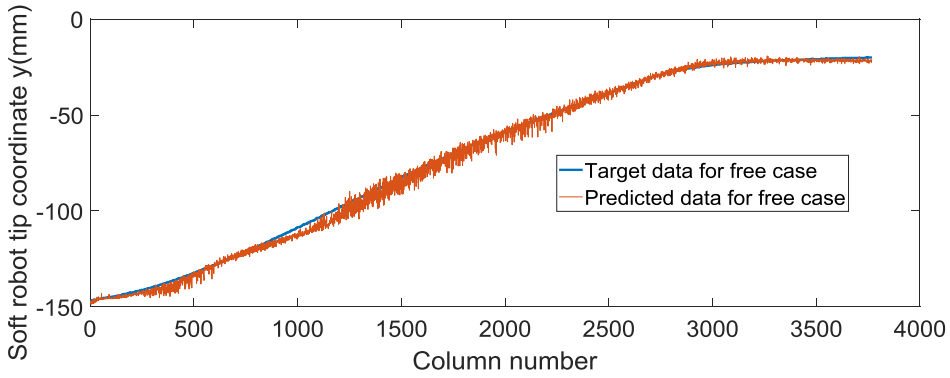

Figure 33: Target data for free case vs Predicted data obtained

It is seen that the network is able to predict the soft robot tip position for all of the obstacle cases. However, there is noise in the prediction which is due to noise present already in the sensor inputs. The reduction in the noise and giving the training data part by part can improve the prediction.

The trained model can be implemented in the controller. By giving real time inputs of curvature sensor and pressure sensor to the trained model, it will be able to predict the soft robot tip position y, which can also be verified from the ground truth vision system.

5.2 Finding Instance of Obstacle Touch

In order to choose an appropriate machine algorithm tool it is necessary to define the type of problem. In this case, the algorithm should be able to learn the trend . Thus, a pattern is to be identified for the different sensor readings corresponding to a particular type of obstacle location making this a pattern recognition problem. The ***Classifier app*** in Matlab rightly serves the purpose. This app comprises of various classifier models, which can be trained to classify the data as required.

5.2.1 Training the sensor data

The curvature and pressure sensor readings recorded earlier are used as training data. These readings are stored in a workspace variable '***inputData'***. After this, another variable is created named '***targetData***' where the associated classifying label is put. The obstacle location 'coordinate y' is used as the classifying label. After this, the values in inputData and targetData are converted into table and stored in a variable '***detectHit***'. The dataset comprises 179442 observations each of free, base, mid, tip making a total of 717768 observations.

Workspace variable name	Data stored		
inputData	Curvature sensor reading, pressure sensor reading		
targetData	Obstacle location coordinate y in mm		
	Base	**Mid**	**Tip**
	-75mm	**-88mm**	**-110mm**
detectHit	Table that stores the whole dataset		

Table 9: Data given to Classifier model for learning

Column Number	Curvature sensor reading	Pressure sensor reading	Class label
1	V_{free}	P_{free}	-19
2	V_{free}	P_{free}	-19
3	V_{free}	P_{free}	-19
.	.	.	.
.	.	.	.
.	.	.	.
	V_{base}	P_{base}	-75
	V_{base}	P_{base}	-75
179442	V_{base}	P_{base}	-75
179443	V_{free}	P_{free}	-19
	V_{free}	P_{free}	-19
	V_{free}	P_{free}	-19
.	.	.	.
.	.	.	.
.	.	.	.
	V_{mid}	P_{mid}	-88
	V_{mid}	P_{mid}	-88
358884	V_{mid}	P_{mid}	-88
358885	V_{free}	P_{free}	-19
	V_{free}	P_{free}	-19
	V_{free}	P_{free}	-19
.	.	.	.
.	.	.	.
.	.	.	.
	V_{tip}	P_{tip}	-110
	V_{tip}	P_{tip}	-110
538326	V_{tip}	P_{tip}	-110
538326	V_{free}	P_{free}	-19
	V_{free}	P_{free}	-19
717768	V_{free}	P_{free}	-19

Table 10: Division of the dataset given to the Classifier model

The table is loaded into the classifier app, which selects the **predictors** and **responses**. In this case, the curvature sensor and pressure sensor readings are used as predictors and the obstacle y coordinates as response.

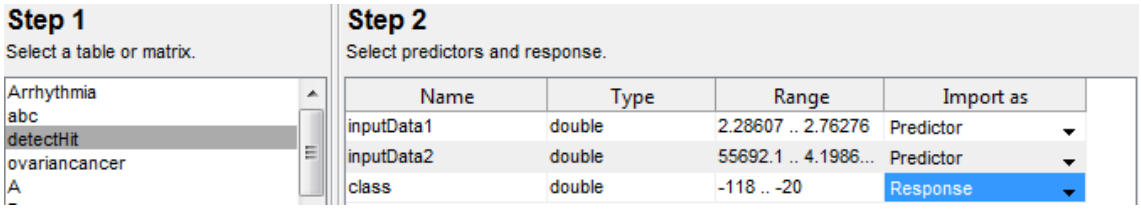

Figure 34: Selection of predictor and response

The scatter plot appears once the session is started. **Figure 36** shows the plot of Pressure (inputData1) vs Curvature sensor reading (inputData2).

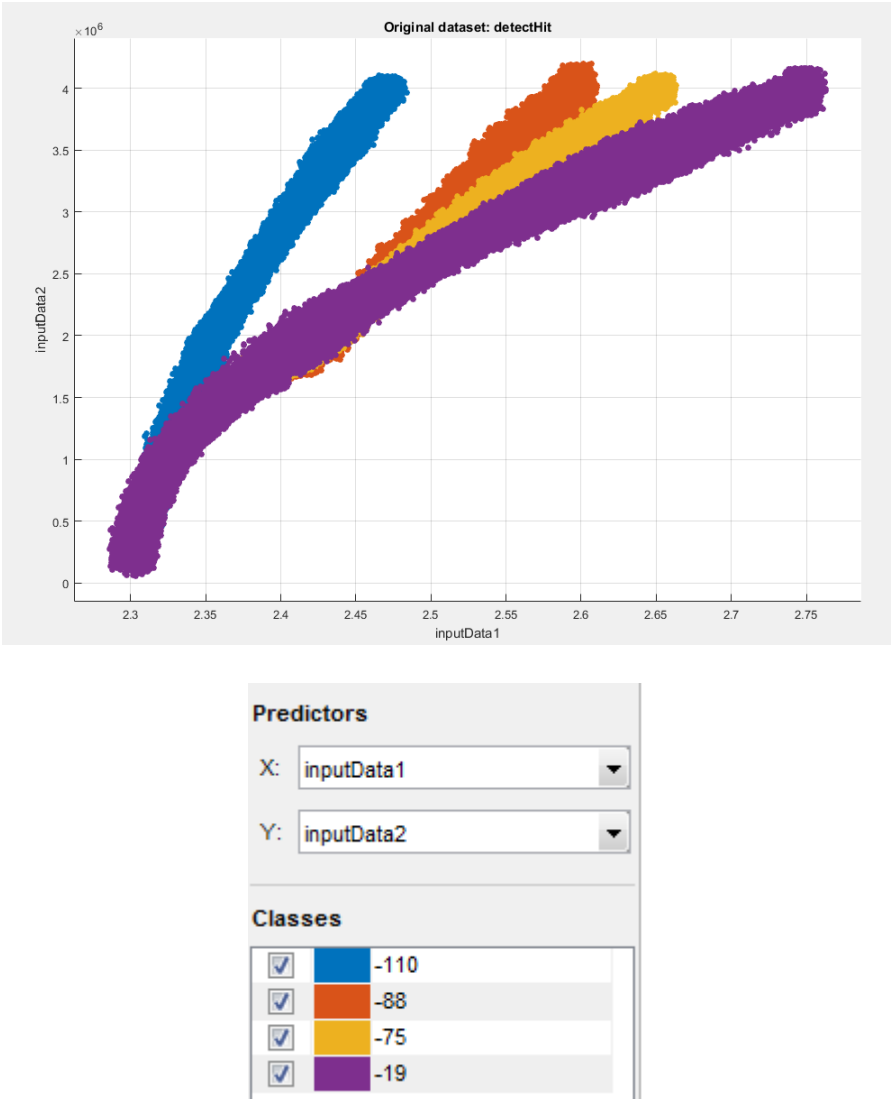

Figure 35: Scatter plot for pressure vs curvature sensor voltage

Now, there are different classifying model options, which can be chosen. To find the best option All Quick train is selected which applies all the models and the best one is selected depending on the accuracy. In this, the classifying model giving the best accuracy is ***Coarse KNN model*** as shown below.

Figure 36: Selected classifier model

The efficiency of this classifier can be understood through the **confusion matrix** and **ROC curve.** The confusion matrix shows how much percent of readings are misclassified and classified for a particular class. The green boxes show correctly classified readings and pink show incorrect ones. From the Figure it is observed that the mid and base are classified with almost similar %, whereas the tip dataset is classified 98% correctly. The interpretation of ROC is that, the more the curve is towards the left corner and in 90 deg the more correctly is the data classified. The ROC Figures show that the model gives the best classsification for tip dataset.

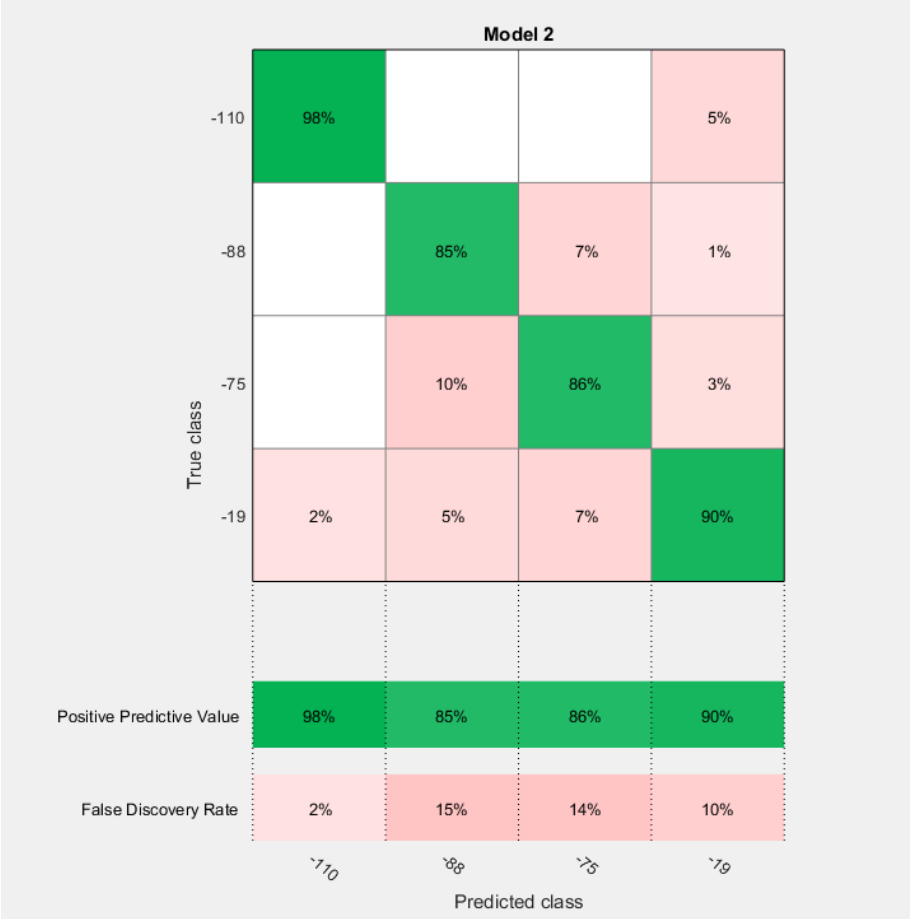

Figure 37: Confusion Matrix

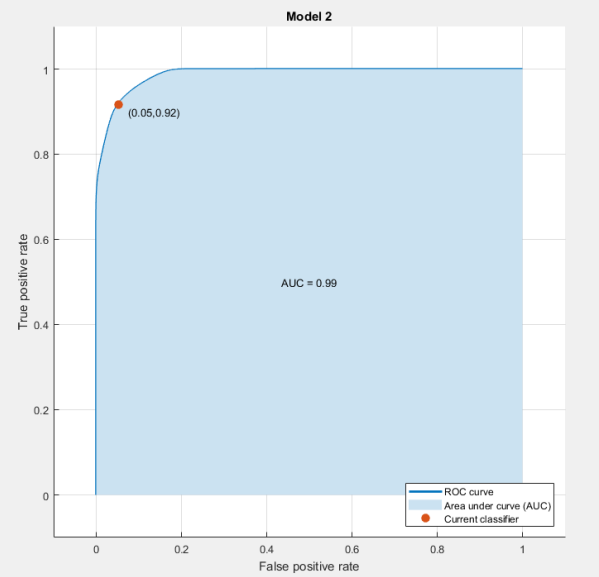

Figure 38: ROC for free obstacle

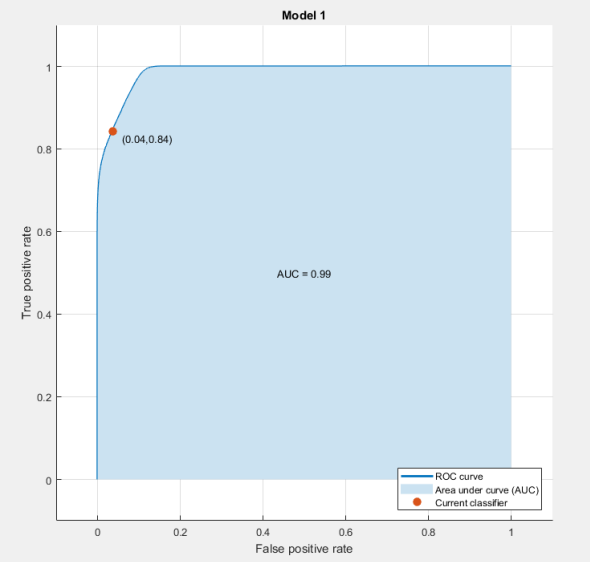

Figure 39: ROC for base obstacle

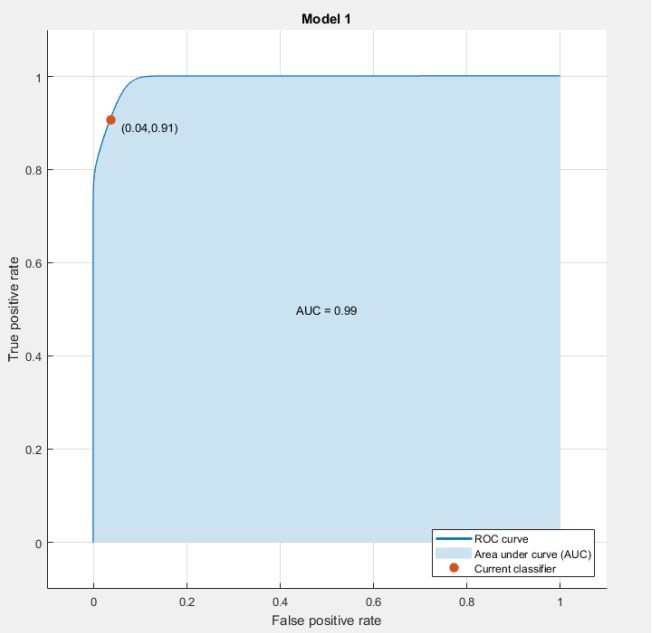

Figure 40: ROC for mid obstacle

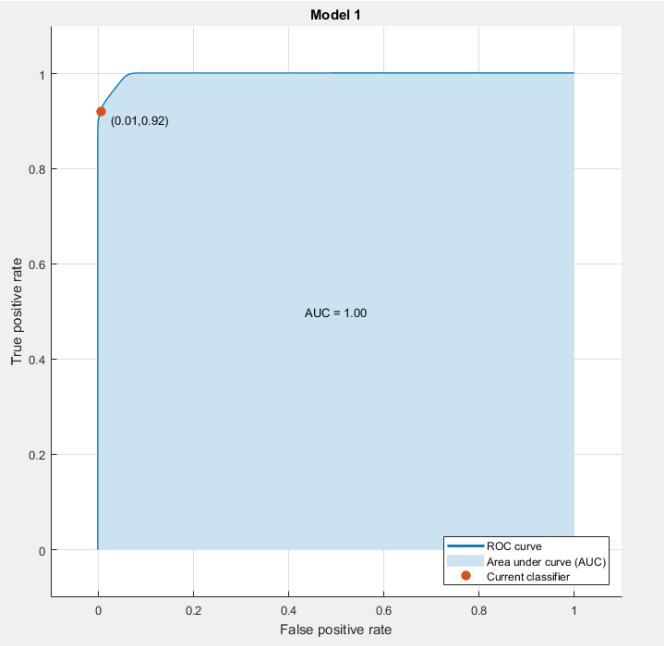

Figure 41: ROC for tip case

5.2.2 Testing data on trained model

The below function obtained is used to check the test data.

```
yfit = trainedModel_obstacleDetection.predictFcn(detectHit)
```

where,
`trainedModel_obstacleDetection` = the trained classifier model which is used to train new data

On running the trained model the answer is stored in the variable **yfit**.For testing purpose the same data for three obstacle cases(base, mid, tip) is considered. Initially the curvature and pressure reading for base case is given as test data input to observe the resulting predicted data of obstacle location. The same test is repeated next time for mid and then for tip case. The obtained results of the trained model for all the cases are explained through graphs below.

The below **Figure 42** shows the **output plot** obtained from trained model on giving the curvature and pressure data as input for **base case**. The target data for base case comprises of **19.9 % free data** and **80.7%** data after the **obstacle** is **hit.** The numbers in circle are markers used to explain the reasons for the different sections of obstacle locations observed.

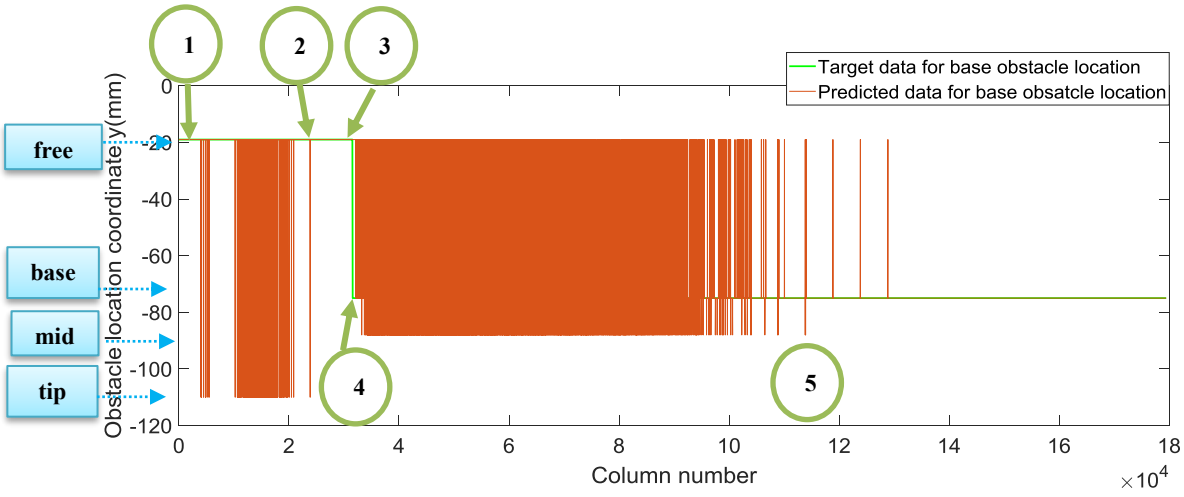

Figure 42: Target data vs predicted data for base obstacle location y (-75 mm)

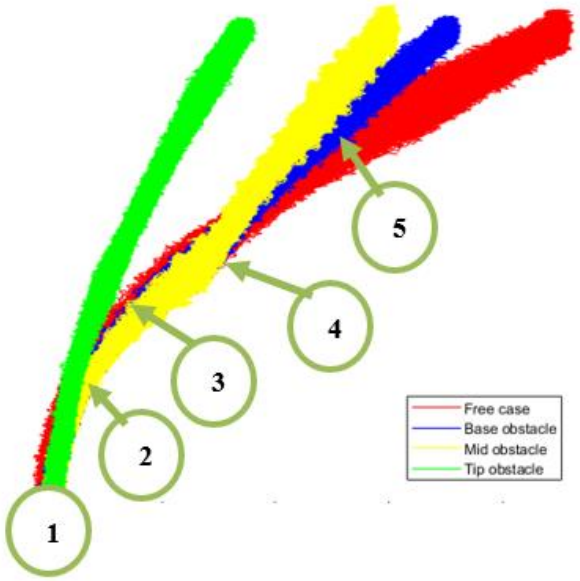

Figure 43: Reference to identify the overlap areas

By analyzing the above two Graphs the below Table is deduced.

Markers	**Target location**	**Predicted locations**	**Reasons for deviation**
1 to 2	-19mm	-19mm, -110mm	The region 1 to 2 is free but tip values appear because it overlaps tip obstacle target values
2 to 3	-19mm	-19mm	This shows that the tip obstacle no more overlaps, and now the graph continues to follow the free case
4	-75mm	-19mm, -75mm	The instance where the obstacle is hit
4 to 5	-75mm	-19mm, -75mm, -88mm	Even after obstacle is hit it takes some time for the sensor readings to change During this period, the graph follows the free case and overlaps with the mid obstacle target values
5 to end	-75mm	-75mm	After this point the base obstacle can be reliably detected

Table 11: Analysis for predicted base obstacle data

It is observed from the above **Table and Figure,** that the base obstacle detection is predicted after **57%** of the obstacle detected data is crossed.

The below **Figure 44** shows the **output plot** obtained from trained model on giving the curvature and pressure data as input for **mid case**. The target data for mid case comprises of **17.2 % free data** and **82.7%** data after the **obstacle** is **hit.**

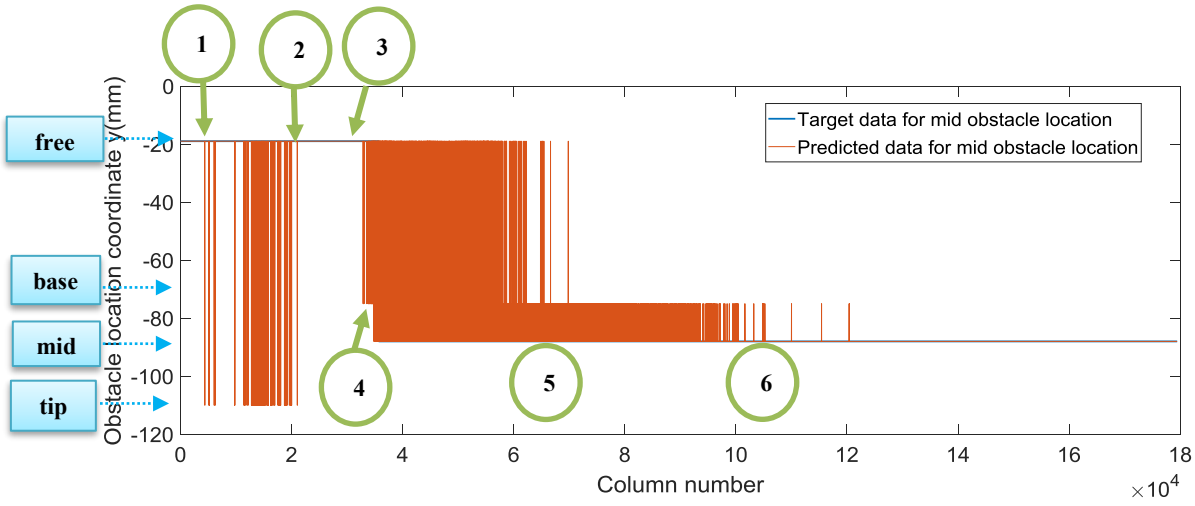

Figure 44: Target data vs predicted data for mid obstacle location y (-88 mm)

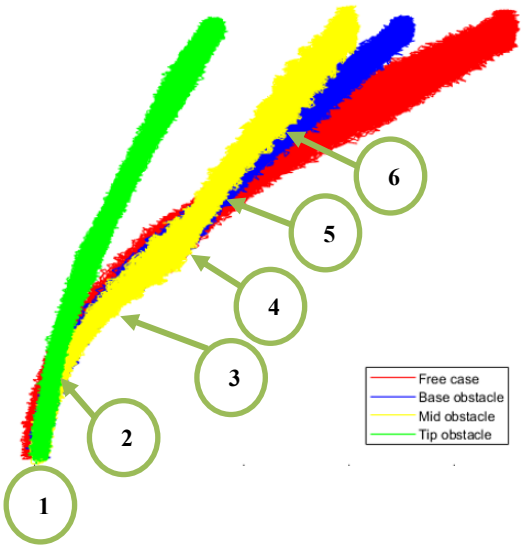

Figure 45: Reference to identify the overlap areas

By analyzing the above two Graphs the below Table is deduced.

Markers	**Target location**	**Predicted locations**	**Reasons for deviation**
1 to 2	-19mm	-19mm, -110mm	The region 1 to 2 is free but tip values appear because it overlaps tip obstacle target values
2 to 3	-19mm	-19mm	This shows that the tip obstacle no more overlap, and now the graph continues to follow the free case
4	-88mm	-19mm, -88mm	The instance where the obstacle is hit
4 to 5	-88mm	-19mm, -75mm, -88mm	Even after obstacle is hit it takes some time for the sensor readings to change During this period, the graph follows the free case and overlaps with the base obstacle target values
5 to 6	-88mm	-88mm, -75mm	Now, there is no more free case overlapping
6 to end	-88mm	-88mm	After this point the mid obstacle can be reliably detected

Table 12: Analysis for predicted mid obstacle data

It is calculated from the above **Graph,** that the mid obstacle detection is predicted after **51%** of the obstacle detected data is crossed.

The below **Figure 46** shows the **output plot** obtained from trained model on giving the curvature and pressure data as input for **tip case**. The target data for tip case comprises of **2.2 % free data** and **97.7%** data after the **obstacle** is **hit.**

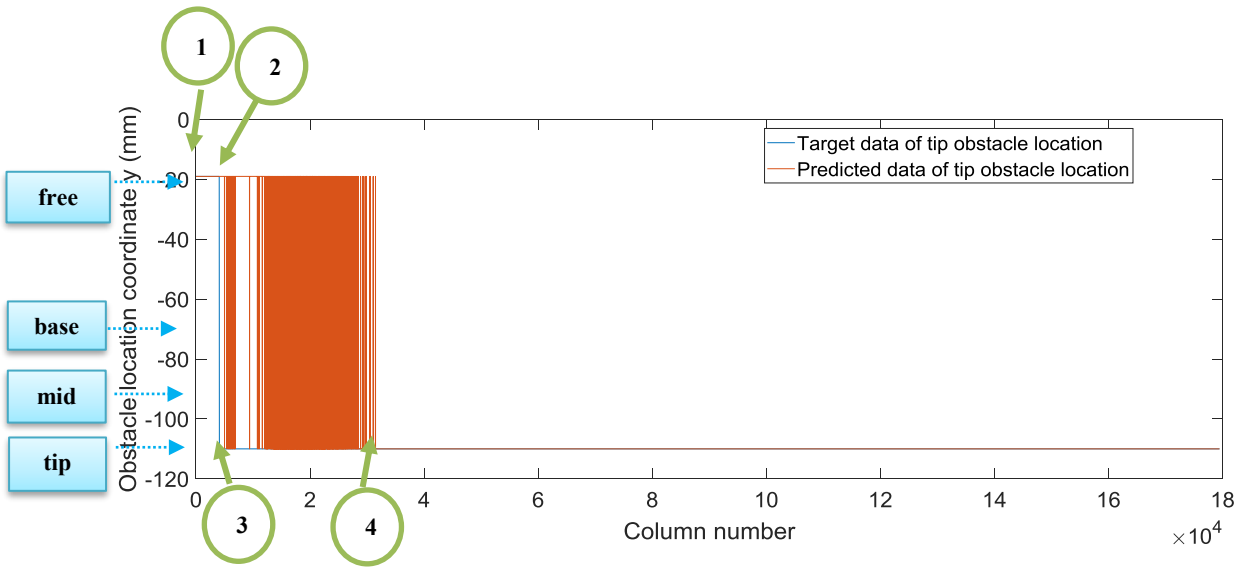

Figure 46: Target data vs Predicted data for tip obstacle y (-110mm)

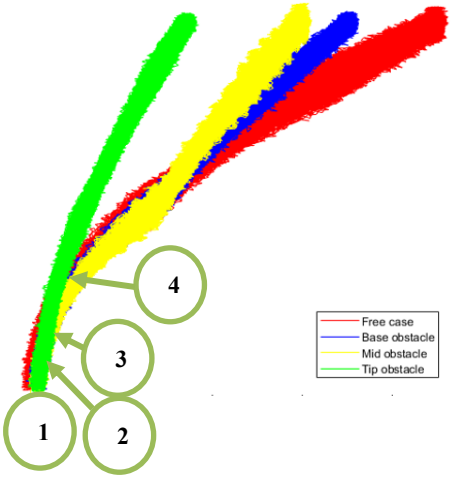

Figure 47: References to identify overlap areas

By analyzing the above two Graphs the below Table is deduced.

Markers	Target location	Predicted locations	Reasons for deviation
1 to 2	-19mm	-19mm	The region 1 to 2 is free
3	-110	-19mm, -110	The instance where the obstacle is hit
3 to 4	-110mm	-19mm, -110mm	The graph follows the free case for some time
4	-110mm	-110mm	After this point the tip obstacle can be reliably detected

Table 13: Analysis for predicted tip obstacle data

It is calculated from the above **Graph,** that the tip obstacle detection is predicted after **16%** of the obstacle detected data is crossed.

Obstacle name	Percent of target obstacle values after which predicted data can be reliably detected
Base	57%
Mid	51%
Tip	16%

Table 14: Probability of getting reliable data for each obstacle case

The analysis done for the predicted data obtained for the different test cases gives following inferences:

1. The more the obstacle towards the tip, more are the chances of obtaining reliable information about hitting.
2. Because the base and the mid obstacle locations were just 13 mm apart, the readings were almost similar causing the overlap of data
3. The other reason for the overlap of data is the noisy readings from the sensor
4. In case of reduction of noise in the curvature sensor data and the pressure sensor the overlap can be reduced and it is possible to detect the smaller gaps in the obstacle locations as 13mm for mid and base in this case
5. The changes in the sensor values after the obstacle hit are not abrupt. The values **follow the free case** for certain time as shown by the percentages above before actually showing a visible change.

6 CONCLUSION

The aim of this research was the study of sensor to determine the state of the fibre reinforced fluidic soft robot. The large DOF and non-linear material property makes it difficult to model the soft robot, unlike the traditional robot counterpart. It was understood from the literature studies that the soft robots position is determined using the PCC concept. However, if the robot is desired to be having non-constant behavior then it would be required to attach sensor at every section of the robot. This can lead to embedding challenges and add more weight to the robot. Instead, this research tried to solve the problem by learning the sensor data through machine learning algorithms. For this, initially an extensive literature study was done for the curvature sensors. There were many good sensors but they were either difficult to manufacture or difficult to attach to the soft robot. The factors important for soft robot sensing were identified as application of use, material and fabrication method of the soft robot, actuator type, embedding, and signal conditioning effect. Considering these factors flex sensor(SpectraSymbol) , bend sensor(Flexpoint) and silver ink stretchable sensor were tested. The bend sensor and stretch sensor added difficulties in attachment due to the signal conditioning (wires &wide base) and sensor construction (fragile base). Hence, it was decided to use the commercially available flex sensor as a curvature sensor for the studied robot because of its lightweight, robustness, cheap and possibility of appropriate attachment.

After this, the curvature sensor is calibrated for bending angle & soft robot tip y (both from vision system)vs curvature voltage. Later, experiments are performed for the soft robot using a screw drilled into a board as obstacle. There are four cases with one being free soft robot movement and the other with different obstacle locations named as base, mid, tip along the curvature sensor length. The readings of pressure from the pressure sensor inside the soft robot, curvature sensor reading and the soft robot tip coordinate y from the vision system are collected. The plots of pressure vs curvature sensor reading for all these four cases shows that there is possibility to identify the presence of obstacle in the path of soft robot. The change in the sensor readings is not abrupt and every case continues to follow the free case before showing visible changes. Machine learning models are used to learn this data.

In order to do this two ways are discussed. In one method, Neural network is used to predict the soft robot tip position ‘y’, given the curvature and pressure sensor reading as input. The network model is able to determine the tip positions for all the four cases, but with presence of some noise. In second method, Classifier app from Matlab is used to identify at what instance the obstacle is hit and which is that obstacle location. It is observed that the tip data is classified 98% correctly. This also reflects when the three test cases of base, mid, tip are tried. The base data is recognized after 57% of sensor data is

already crossed. Mid data can be recognized after 51%. However, the tip shows best efficiency of being recognized with 16% data crossing after obstacle is actually hit.

The clear reasons are that because mid and base are placed very closely they follow almost the same trend. This suggests that if any application requires the presence of some obstacle at closer location the flex sensor would be not an appropriate option as a curvature sensor. Although if the obstacles are located at appreciable distance apart for e.g. the base and the tip case only, then flex sensor can work as a good sensor.

The vibrations in the soft robot during actuation if minimized can result into finer values from pressure sensor data. Further, noise reductions in the curvature sensor can result into finer curves enabling less overlap of data after the obstacle is hit. By considering more number of obstacles along the length, the analysis can be done more better. The alternative Mask deposition technique [42] in EGaIn fabrication can be a good candidate for curvature sensor.

Application wise, same experiments can be applied to a soft robot for hand. Soft robot hand with sensors embedded can be tested on a 3D printed hand resembling the patient hand. The screw used in the experiments done in this thesis can be considered as the knuckles of the hand. Similar experiments as performed here can be carried out to find the sensor values for each digit of the hand by opening and closing it. Each digit would give sensor value based on the knuckle position. A vision system can be used for the position calibration.

The research carried out gives a way to analyze the soft robot, where there are known obstacle scenarios for which experiments can be carried out to learn a model and the robot state can be determined.

REFERENCES

[1] J. Hughes, U. Culha, F. Giardina, F. Günther, and A. Rosendo, "Soft Manipulators and Grippers: A Review," *Front. Robot. AI*, vol. 3, no. November, pp. 1–12, 2016.

[2] C. Laschi and B. Mazzolai, "Lessons from Animals and Plants," *IEEE Robot. Autom. Mag.*, no. September, pp. 107–114, 2016.

[3] E. Guizzo, "Soft robotics," vol. 17, no. 6, pp. 756–757, 2012.

[4] "Kuka Robots." [Online]. Available: https://www.active8robots.com/robots/kuka-robots/. [Accessed: 08-Sep-2017].

[5] E. Demaitre, "robotics business review," 2015.

[6] N. Elango and A. A. M. Faudzi, "A review article: Investigations on soft materials for soft robot manipulations," *Int. J. Adv. Manuf. Technol.*, vol. 80, no. 5–8, pp. 1027–1037, 2015.

[7] B. S. Homberg, R. K. Katzschmann, M. R. Dogar, and D. Rus, "Haptic Identification of Objects using a Modular Soft Robotic Gripper."

[8] D. Rus and M. T. Tolley, "Design, fabrication and control of soft robots," *Nature*, vol. 521, no. 7553, pp. 467–475, 2015.

[9] R. Deimel and O. Brock, "A novel type of compliant and underactuated robotic hand for dexterous grasping," *Int. J. Rob. Res.*, vol. 35, no. 1–3, pp. 161–185, 2016.

[10] B. Mosadegh *et al.*, "Pneumatic networks for soft robotics that actuate rapidly," *Adv. Funct. Mater.*, vol. 24, no. 15, pp. 2163–2170, 2014.

[11] K. C. Galloway, P. Polygerinos, C. J. Walsh, and R. J. Wood, "Mechanically programmable bend radius for fiber-reinforced soft actuators," *2013 16th Int. Conf. Adv. Robot. ICAR 2013*, 2013.

[12] C.-P. Chou and B. Hannaford, "Measurement and Modeling of McKibben Pneumatic Artificial Muscles," *Ieee Trans. Robot. Autom.*, vol. 12, no. 1, pp. 90–102, 1996.

[13] C. Keplinger, T. Li, R. Baumgartner, Z. Suo, and S. Bauer, "Harnessing snap-through instability in soft dielectrics to achieve giant voltage-triggered deformation," *Soft Matter*, vol. 8, no. 2, pp. 285–288, 2012.

[14] C. Laschi, "An octopus points the way to soft robotics," 2017.

[15] "Soft Robotics>Translational applications." [Online]. Available:

https://biodesign.seas.harvard.edu/soft-robotics. [Accessed: 02-Sep-2017].

[16] "Artificial eyelid closure using soft exopatches." [Online]. Available: https://softroboticstoolkit.com/book/artificial-eyelid-closure-using-soft-exopatches. [Accessed: 02-Sep-2017].

[17] A. Swiss, "YouGrabber – playful therapy for fi nger, hand and arm rehabilitation ®."

[18] "Soft robot helps the heart beat." [Online]. Available: https://www.seas.harvard.edu/news/2017/01/soft-robot-helps-heart-beat.

[19] "Our Product." [Online]. Available: https://www.softroboticsinc.com/our-products/. [Accessed: 02-Sep-2017].

[20] R. J. Webster and B. a. Jones, "Design and Kinematic Modeling of Constant Curvature Continuum Robots: A Review," *Int. J. Rob. Res.*, vol. 29, no. 13, pp. 1661–1683, 2010.

[21] C. Lee *et al.*, "Soft robot review," *Int. J. Control. Autom. Syst.*, vol. 15, no. 1, pp. 3–15, 2017.

[22] P. Li, Z. Yan, K. Zhou, L. Zhang, and J. Leng, "Monitoring static shape memory polymers using a fiber Bragg grating as a vector-bending sensor," *Opt. Eng.*, vol. 52, no. 1, p. 14401, 2013.

[23] J. Ge, A. E. James, L. Xu, Y. Chen, K. Kwok, and M. P. Fok, "Bidirectional Soft Silicone Curvature Sensor Based on Off-Centered Embedded Fiber Bragg Grating," vol. 28, no. 20, pp. 2237–2240, 2016.

[24] M. Kreuzer, "Strain measurement with fiber bragg grating sensors," *HBM, Darmstadt, S2338-1.0 e*, 2006.

[25] H. Wang, S. Member, R. Zhang, W. Chen, X. Liang, and R. Pfeifer, "Short Papers Fiber Bragg Gratings," vol. 21, no. 6, pp. 2977–2982, 2016.

[26] C. To, T. L. Hellebrekers, and Y. L. Park, "Highly stretchable optical sensors for pressure, strain, and curvature measurement," *IEEE Int. Conf. Intell. Robot. Syst.*, vol. 2015–Decem, pp. 5898–5903, 2015.

[27] U. Tata, H. Cao, C. M. Nguyen, and J. Chiao, "Flexible sputter-deposited carbon strain sensor.pdf," vol. 13, no. 2, pp. 444–445, 2013.

[28] J. Suikkola *et al.*, "Screen-Printing Fabrication and Characterization of Stretchable Electronics," *Sci. Rep.*, vol. 6, no. 1, p. 25784, 2016.

[29] “Flex Sensors.” [Online]. Available: http://www.spectrasymbol.com/product/flex-sensors/. [Accessed: 09-Feb-2017].

[30] “Flexpoint-Flexible Sensor Systems.” [Online]. Available: http://www.flexpoint.com/. [Accessed: 18-Nov-2017].

[31] D. H. Kim, S. W. Lee, and H. S. Park, “Sensor evaluation for soft robotic hand rehabilitation devices,” *Proc. IEEE RAS EMBS Int. Conf. Biomed. Robot. Biomechatronics*, vol. 2016–July, pp. 1220–1223, 2016.

[32] A. Pascual-Leone, “Design considerations for a wearable monitor to measure finger posture,” *J. Neuroeng. Rehabil.*, vol. 2, p. 5, 2005.

[33] S. Rosset and H. R. Shea, “Flexible and stretchable electrodes for dielectric elastomer actuators,” *Appl. Phys. A Mater. Sci. Process.*, vol. 110, no. 2, pp. 281–307, 2013.

[34] T. Yamada *et al.*, “A stretchable carbon nanotube strain sensor for human-motion detection,” *Nat. Nanotechnol.*, vol. 6, no. 5, pp. 296–301, 2011.

[35] A. Firouzeh, A. Foba Amon-Junior, and J. Paik, “Soft piezoresistive sensor model and characterization with varying design parameters,” *Sensors Actuators A Phys.*, vol. 233, pp. 158–168, 2015.

[36] H. A. Wurdemann *et al.*, “Embedded electro-conductive yarn for shape sensing of soft robotic manipulators,” *Proc. Annu. Int. Conf. IEEE Eng. Med. Biol. Soc. EMBS*, vol. 2015–Novem, pp. 8026–8029, 2015.

[37] M. Haghshenas-Jaryani, W. Carrigan, C. Nothnagle, and M. B. J. Wijesundara, “Sensorized soft robotic glove for continuous passive motion therapy,” *Proc. IEEE RAS EMBS Int. Conf. Biomed. Robot. Biomechatronics*, vol. 2016–July, pp. 815–820, 2016.

[38] A. Firouzeh and J. Paik, “The Design and Modeling of a Novel Resistive Stretch Sensor with Tunable Sensitivity,” *IEEE Sens. J.*, vol. 15, no. 11, pp. 6390–6398, 2015.

[39] Y.-L. Park, B. Chen, and R. J. Wood, “Design and Fabrication of Soft Aftificial Skin using Embedded Microchannels and Liquid Conductors,” *IEEE Sens J.*, vol. 12, no. 8, pp. 2711–2718, 2012.

[40] M. D. Dickey, R. C. Chiechi, R. J. Larsen, E. A. Weiss, D. A. Weitz, and G. M. Whitesides, “Eutectic gallium-indium (EGaIn): A liquid metal alloy for the formation of stable structures in microchannels at room temperature,” *Adv. Funct. Mater.*, vol. 18, no. 7, pp. 1097–1104, 2008.

[41] T. C. Searle, K. Althoefer, L. Seneviratne, and H. Liu, “An optical curvature sensor

for flexible manipulators," *Proc. - IEEE Int. Conf. Robot. Autom.*, pp. 4415–4420, 2013.

[42] R. K. Kramer, C. Majidi, and R. J. Wood, "Masked deposition of gallium-indium alloys for liquid-embedded elastomer conductors," *Adv. Funct. Mater.*, vol. 23, no. 42, pp. 5292–5296, 2013.

[43] J. T. Muth *et al.*, "Embedded 3D printing of strain sensors within highly stretchable elastomers," *Adv. Mater.*, vol. 26, no. 36, pp. 6307–6312, 2014.

[44] P. Manandhar, P. D. Calvert, and J. R. Buck, "Elastomeric ionic hydrogel sensor for large strains," *IEEE Sens. J.*, vol. 12, no. 6, pp. 2052–2061, 2012.

[45] S. K. Yildiz, R. Mutlu, and G. Alici, "Performance quantification of strain sensors for flexible manipulators," *IEEE/ASME Int. Conf. Adv. Intell. Mechatronics, AIM*, vol. 2016–Septe, pp. 584–589, 2016.

[46] S. Ozel *et al.*, "A Composite Soft Bending Actuation Module with Integrated Curvature Sensing," pp. 4963–4968, 2016.

[47] S. Ozel, N. A. Keskin, D. Khea, and C. D. Onal, "A precise embedded curvature sensor module for soft-bodied robots," *Sensors Actuators, A Phys.*, vol. 236, pp. 349–356, 2015.

[48] "Edward Sensor Hands:The Techno Gloves." [Online]. Available: http://emerald.tufts.edu/programs/mma/emid/projectreportsS04/hamalainen.html. [Accessed: 02-Sep-2017].

[49] "How to Make a Remote Controlled Robotic Hand with Arduino." [Online]. Available: https://create.arduino.cc/projecthub/Gabry295/how-to-make-a-remote-controlled-robotic-hand-with-arduino-32b0f5. [Accessed: 02-Sep-2017].

[50] "Smart Glove Turn Sign Language Gestures into Vocalized Speech." [Online]. Available: https://singularityhub.com/2012/09/16/smart-gloves-turn-sign-language-gestures-into-vocalized-speech/. [Accessed: 02-Sep-2017].

[51] "DIY 10-finger flex sensor gloves for possible VR or video game control." [Online]. Available: http://benkrasnow.blogspot.fi/2010/12/diy-10-finger-flex-sensor-gloves-for.html. [Accessed: 02-Sep-2017].

[52] "SudoGlove: Bend index finger to accelerate car." [Online]. Available: https://www.cnet.com/news/sudoglove-bend-index-finger-to-accelerate-car/. [Accessed: 02-Sep-2017].